4

Fixed and Floating Offshore Wind Turbine Support Structures

Erin E. Bachynski

CHAPTER MENU

4.1 Introduction

Compared to onshore wind turbines, the support structure – considered here to be the part of the load-bearing structure that is below the lower flange of the tower – is a component that is unique to the offshore environment. Support structures for offshore wind turbines (OWTs) take various shapes and forms, depending on the water depth, turbine size, geotechnical aspects and environmental conditions. In shallow water (<40–60 m), bottom-fixed structures such as monopiles, gravity-based structures or jackets are typically used. An overview of bottom fixed support structures is given in Section 4.2. In deeper water, floating support structures may be more economically feasible. Although the majority of commercial offshore turbines are supported by

Offshore Wind Energy Technology, First Edition. Olimpo Anaya-Lara, John O. Tande, Kjetil Uhlen, and Karl Merz.

Companion website: www.wiley.com/go/tande/offshore-wind-energy

bottom-fixed structures, several large-scale floating wind turbine prototypes have already been installed and successfully operated for several years. An overview of common and novel floating support structures is given in Section 4.3.

The support structure of an OWT must be designed to withstand actions from the air, sea and soil, as well as those from the turbine itself, during the intended service lifetime, typically 25 years. The basic design considerations are summarized in Section 4.4. Section 4.5 examines the conceptual design phase of OWT support structures: overall sizing considerations and upscaling laws, preliminary analysis methods and initial optimization. In order to further develop the design, a more thorough understanding of the loads (Section 4.6) is needed. An overview of the wind and wave conditions and load effects is presented in this chapter, while more in-depth references for aerodynamic and hydrodynamic load calculations are suggested for detailed study.

Finally, Section 4.7 discusses numerical and experimental global analysis methods for OWTs. The support structure behaviour is tightly coupled with the wind turbine and its design requires consideration of the system as a whole. Numerical aero-hydro-servo-geo-elastic analysis tools have been developed to better understand the behaviour of these complex systems. Experimental campaigns that give deeper insight into the physical loads and responses have a complementary role for concept verification and the validation of numerical tools.

4.2 Bottom-fixed Support Structures

The vast majority of installed OWTs to date are located in relatively shallow water, where 'bottom-fixed' solutions can be applied (Figure 4.1). Such support structures are characterized by a high degree of fixity at the seabed, which places all natural frequencies of the complete OWT system above the typical wave frequencies. The static stability of the system is provided by interaction between the soil and foundation. Typical methods of achieving this high degree of fixity include driving piles through the seabed (i.e. monopole, tripod, jacket), establishing and maintaining a significant pressure differential (i.e. suction bucket), or taking advantage of the gravitational force (i.e. gravity-based structure). Characteristics, trends, and challenges for these foundation types are discussed separately below.

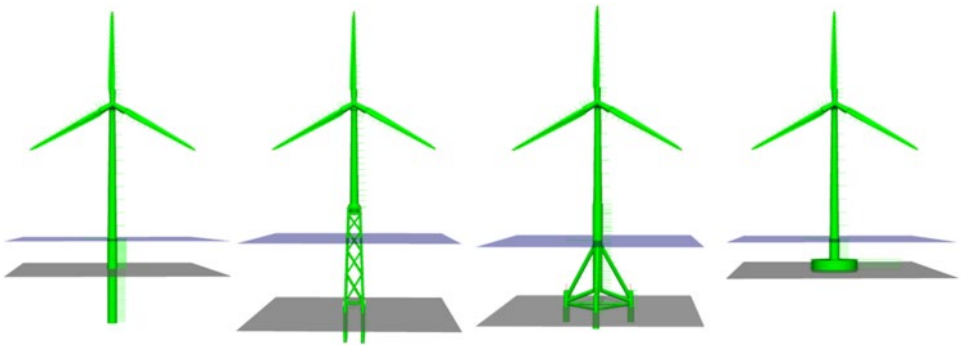

Figure 4.1 Bottom-fixed support structures (l–r): monopile, tripod, jacket, gravity-based structure.

Monopile, tripod and jacket wind turbines are examples of pile-supported structures. All of these are typically built from steel and their installation requires pile-driving: driving a vertical pile into the seabed using a hydraulic hammer, steam or drilling into rock. This process – particularly hammering – may be noisy and local restrictions on the allowable noise may be critical, particularly for large monopiles.

As the name suggests, monopile foundations consist of a single cylindrical pile hammered into the seabed. Monopiles are the most common offshore support structure, accounting for 80.1% of installed OWTs in Europe by the end of 2015 (EWEA, 2016). The key advantages of monopile support structures are their simple geometry – both for design and manufacturing – as well as the extensive industry experience. As the industry moves toward higher wind turbine ratings, the size of monopiles is increasing correspondingly. For example, at Sherringham Shoal, with 3.6-MW turbines, the diameter is up to 5.2 m, with pile embedment lengths below the seabed up to 37 m (Sherringham Shoal, 2012), while the Dudgeon project (6-MW turbines) makes use of diameters up to 7.4 m (Dudgeon Offshore Wind Farm, 2014). The selection of the pile diameter, thickness and length depends on the local environmental conditions, such as the water depth, soil stiffness and metocean conditions. Critical design considerations for monopiles include the tolerances for displacement and rotation at the mudline, desired structural natural frequency of the complete wind turbine structure, fatigue – especially in the pile itself (5–20 m below the mudline) – and wave loads in extreme conditions.

The increasing diameter of monopile support structures – as well as the trends towards exploiting the wind resource in deeper water – presents some interesting research challenges. On the geotechnical side, cyclical loading on large diameter piles requires better understanding and design procedures for soil–structure interaction compared to the oil and gas industry (Doherty *et al*., 2011). Furthermore, especially as the monopile diameter increases, the importance of nonlinear wave loading in steep and breaking wave conditions is an increasing concern. Practical and reliable modelling of such loads requires further research into the nonlinearity of the waves themselves as well as the load mechanisms (Bredmose *et al*., 2013). The fatigue and ultimate capacity of the grouted connection between the tower and the monopile is also the subject of active research. Failures in plain grouted connections were observed in installed turbines and the effects of the dynamic moment on grouted connections with shear keys have been seen to be important (Lotsberg, 2013).

Jacket foundations provide potential material (cost) savings through more efficient geometry and greater transparency to wave loads, and are expected to be more cost effective in deeper water than monopiles. The term 'jacket' originates from the structural design close to the seabed: the legs of the truss structure are placed around several piles, like the sleeves of a jacket around a person's arms. The piles can be installed prior to (faster) or after (most common) the installation of the support structure; grouting is used in between the jacket legs and piles. Design challenges for jacket support structures include fatigue in the joints and manufacturability of the structure. The transfer of wind loads, which are traditionally dominant for jacket wind turbines, as well as extreme wave loads, to the support structure and foundation is an important aspect of design analyses (Chakrabarti, 2005). To make jackets more competitive, current research topics include optimization (to achieve lighter or more easily manufactured structures), improved numerical modelling (to account for the structural complexities more

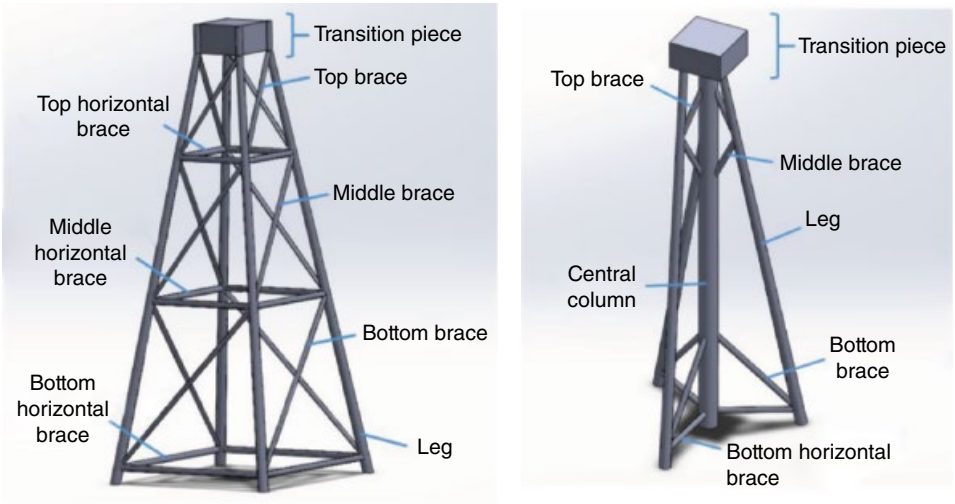

Figure 4.2 Traditional (left) and twisted jacket designs (*Source:* Chen *et al*., 2016. Reproduced with permission of MDPI AG.).

efficiently) and increased accuracy in load predictions (to reduce uncertainties and risk). Figure 4.2 compares a traditional and a twisted jacket foundation, which is a relatively new approach for cost reduction (Chen *et al*., 2016).

Tripod (and quadpod) wind turbine foundations represent, to some extent, a hybrid combination of jacket and monopile support structures. Similar to jackets, tripods and quadpods achieve fixity to the seabed through three or four piled legs, and the wide base allows the overturning moment to be distributed among the legs. Unlike jackets, the structure consists of several large-diameter elements, with a single central column extending through the water surface. These designs are more efficient than monopiles, can be installed with smaller pile-driving equipment than monopiles and have fewer components than jackets. Similar design challenges are observed as for the monopiles and jackets. At present, tripods and quadpods are not widespread, which may be because the manufacturing process is more complex than a monopile and the components are heavier than those of a jacket.

Suction bucket foundations are an alternative to pile-driving, and suction bucket technology has been proposed for both single-column (similar to monopiles) and multicolumn support structures (tripods). Fixity at the seabed is achieved by pumping water out of an upside-down 'bucket' at the seabed. The pressure differential (lower pressure in the bucket and higher pressure on the bucket top) drives the foundation into the seabed. The technology has been used in the oil and gas industry and has been deployed in demonstration projects but has not yet been adopted widely for wind turbines. Suction bucket foundations eliminate the need for noisy pile-driving and can be used on a wide variety of soils, as long as the soil supports penetration of the bucket. Compared to the oil and gas industry, suction buckets for OWTs – especially for monopiles – are larger and need to withstand large overturning moments, which is still a design challenge.

Finally, gravity-based structures (GBSs) provide yet another alternative to pile-driving. As the name suggests, a GBS relies on its weight to stay upright. Heavy ballast is typically placed in a wide base (Figure 4.1), which is connected to a narrower shaft that extends above the waterline. This concept was borrowed early from the oil and gas industry: the first offshore wind farm in Denmark (Vindeby) employed GBSs in 5 m water depth. While GBSs avoid the noisy and demanding piling process, the extra weight does require larger transport vessels and cranes. Design challenges for GBS wind turbines include geotechnical stability – seabed preparation and scour protection may be needed, although GBSs can be used for a variety of soils – as well as cost reduction and extensions to deeper water.

4.3 Floating Support Structures

In contrast to bottom-fixed support structures, floating support structures are generally characterized by greater compliance and they are typically intended for deeper water. Figure 4.3 shows a selection of floating wind turbine concepts, which are moored by catenary lines, taut lines, or tendons.

A common classification of floating wind turbines (FWTs) is based on their primary source of stability: via the waterplane moment of inertia, a very low centre of gravity or via the mooring system. This classification can be illustrated by a general equation for the linear stiffness of a floating structure in pitch:

$$C_{55} + K_{55} = \rho g I_{55} - Mgz_G + \rho g \nabla z_B + K_{55} \tag{4.1}$$

where C_{55} is the hydrostatic stiffness, which is obtained from the waterplane moment of inertia (I_{55}), the dry mass (M) and its vertical centre of gravity (z_G), and the displaced volume (∇) and its centre of buoyancy (z_B). The stiffness obtained from the mooring system is indicated as K_{55}. The waterplane moment of inertia (I_{55}) in pitch (about the y-axis) is obtained by integration over the waterplane area (A_{wp}):

$$I_{55} = \iint_{A_{wp}} x^2 \mathrm{d}x\,\mathrm{d}y. \tag{4.2}$$

Semi-submersible and barge-type FWTs obtain the majority of their stability from I_{55}. In order to increase I_{55}, the most efficient use of material is to increase the area that is far from the central axis, rather than increasing the total area. In a semi-submersible design, the outer columns contribute the most to stability. The use of surface-piercing columns (as in a semi-submersible) rather than a solid flat deck (as in a barge) allows for reduction of the wave forces but requires careful structural design. Squeeze/pry loads and racking moments on the columns must be taken up by a bracing system or within the columns and pontoons of a brace-less design (Chakrabarti, 2005). Compared to other types of FWTs, the installation of semi-submersibles is relatively simple.

Spar FWTs obtain the majority of their stability from the Mgz_G and $\rho g \nabla z_B$ terms in Equation 4.1: the centre of gravity is placed far below the centre of buoyancy, such that the positive restoring force from gravity far exceeds the negative contribution from the buoyancy force. Such a design allows the waterplane area to be quite small, which significantly reduces the wave loads. The main disadvantage of spar FWTs is their deep

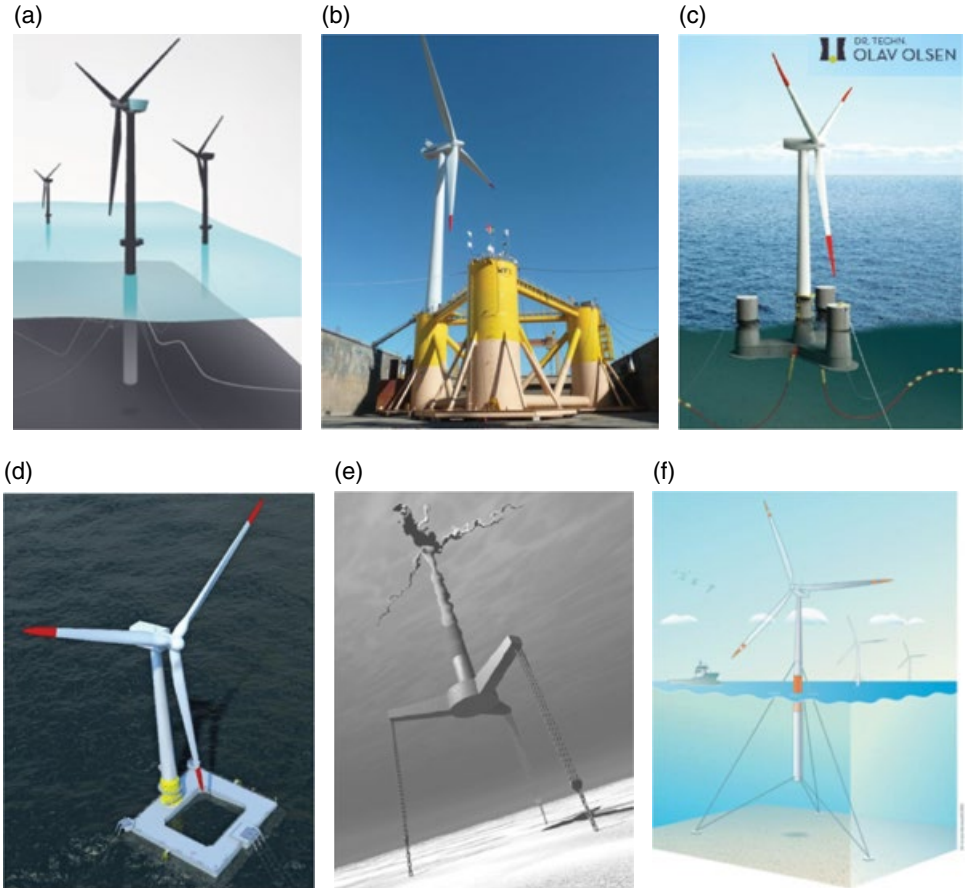

Figure 4.3 Floating wind turbines. (a) Spar: Hywind from Statoil (Statoil, 2011). (b) Semi-submersible: WindFloat from Principle Power (Principle Power, 2011). (c) Semi-submersible: OO Star from Dr techn Olav Olsen (Personal communication with Trond Landbø). (d) Barge: from IDEOL (IDEOL, 2016). (e) TLP: from Glosten (Moon III and Nordstrom, 2010). (f) TLB: from IFE (Nygaard and Myhr, 2014.), Illustrator: Endre Barstad (altkanendres.no).

draft, which limits the possibilities of completing the mating process (connecting the turbine and tower to the hull) onshore and the locations in which they can be installed. An additional consideration for spar wind turbines is that the natural frequencies of heave and pitch (or roll) motions could be similar, which could lead to a Mathieu instability (Faltinsen, 1990).

Tension-leg platform (TLP) and tension-leg buoy (TLB) FWTs use the mooring system to provide the majority of the restoring force. These FWTs are designed such that the buoyancy force exceeds the gravitational force (weight) of the platform and turbine. The mooring system, consisting of n lines or tendons, is under tension. Vertical tendons are associated with TLPs, which are restricted in heave, pitch and roll, while angled tendons are associated with TLBs, which are restricted in all degrees of freedom. TLP and TLB wind turbines offer the advantages of very limited

motions, reduced footprint and potential savings on steel in the hull, but they suffer from the high cost of the mooring system, which must withstand large dynamic loads (and must, typically, avoid loss of tension). The linearized stiffness in pitch of the mooring system of a TLP with n vertical tendons located at radius r and depth z can be estimated as:

$$K_{55} = \sum_{j=1}^{n} \left(\frac{F}{l_0} z^2 + \frac{EA}{l_0} r^2 \right) \cos^2 \theta_j \tag{4.3}$$

where F is the pretension per tendon, l_0 is the unstretched line length, EA represents the axial stiffness of the tendon, and θ_j is the angle of attachment in the horizontal plane.

While steel spar, semi-submersible and tension-leg platforms are the most common research topics today, novel variations on such platforms have also been presented. Azcona *et al.* (2014) and Viselli *et al.* (2014) claim that concrete hulls – particularly for semi-submersible floaters – may be able to reduce the manufacturing cost. V-shaped semi-submersibles, self-stable tension-leg platforms and spar platforms with a single taut mooring line (tension-leg spar) have also been proposed (Botta *et al.*, 2009; Karimirad, 2011; SWAY, 2012; Karimirad and Michailides, 2015).

4.4 Design Considerations

OWTs should be designed for serviceability – that is production of power – and safety – that is absence of accidents – throughout their intended service life, with as low a cost as possible per unit delivered power. The design must first and foremost satisfy certain fundamental criteria in terms of stability and structural integrity. Additional considerations, such as the selection of natural periods or limits on offsets, help to achieve a reasonable design which better meets the functional requirements.

Particular concerns related to stability may arise for FWTs. Evaluation of the hydrostatic stability is a relatively straightforward calculation. Catenary-moored structures must generally satisfy certain requirements for metacentric height, while stability contributions from the mooring system become important for TLPs and TLBs (ABS, 2013; DNV, 2013). According to Masciola *et al.* (2015), dynamic intact stability may be more challenging to assess than static stability. Stability in damaged conditions must also be considered according to current practice. However, since the consequences of failure for an OWT are primarily economical, there is a discussion about to what extent accidental limit state (ALS), and especially damaged stability criteria, should be satisfied.

The structural integrity should be checked to avoid failure due to reaching the maximum structural resistance, that is the ultimate limit state (ULS), or due to cyclic loading, that is fatigue (FLS), or due to accidental loads (ALS), or due to exceeding tolerances for operation (serviceability, SLS). These considerations have been established for offshore structures (Clauss *et al.*, 1982; DNV, 2010b) and are similar for wind turbine support structures except for the effects of the wind turbine (in operational, parked, idling and fault conditions). Due to aerodynamic loading – and, in particular, the behaviour of variable speed variable pitch wind turbines – it is

important to note that extreme environmental conditions may not necessarily correspond to the most extreme loads or load effects, locally or globally. In particular, conditions near the rated wind speed or when the turbine has incurred faults may be critical.

In general, the structural strength evaluation should account for all of the structural components over their individual lifetimes. This includes all components of the support structure (foundation, substructure, mooring system), the power cable and any supporting structure, and all of the components of the wind turbine. Even if the wind turbine and power cable are classified separately from the support structure, a correct analysis requires consideration of the system as a whole, in addition to local analysis of hot spots and stress raisers (such as welds, doorways, or connections). Prior to detailed structural strength evaluation, the determination of load effects is typically carried out according to design standards, which are based on the principle of load and resistance factor design (LRFD) (IEC, 2005, 2008; DNV, 2007, 2013; ABS, 2013).

Surface corrosion is an important concern for the strength of OWTs: support structures are often exposed to the harsh saltwater environment, while the blades are exposed to erosion impacts due to salt particles and water droplets. A combination of cathodic protection, protective coatings and corrosion resistant materials may be considered, according to experience from the offshore oil and gas industry, as described in, for example, NORSOK (2012). The offshore wind industry needs maintenance-free coating systems that can last for 20 years. Life cycle analysis suggests that a zinc duplex (thermally sprayed zinc and paint system) may be a promising solution for the atmospheric zone and splash zone, while the submerged zone should use a combination of cathodic protection and epoxy coating (Bjørgum, 2015). In the future, self-repairing coatings may improve the performance further.

In addition to designing for structural strength and stability, the designed support structure must be producible, installable and accessible. For a structure to be producible, the dimensions of the plating must be formable, weld locations must be accessible (and, ideally, possible to inspect) and the overall dimensions of components that are to be installed separately must fit within a shipyard or dry dock. Installation requirements must also be taken into account at an early stage in the design process. An offshore wind farm often consists of hundreds of structures and the installation costs may represent a significant portion (11–20%) of the total investment cost (Moné *et al*., 2015a, 2015b). Finally, access to the turbine for inspections or maintenance is an additional consideration that may affect the design. Access platforms on bottom-fixed wind turbines must, for example, be placed high enough to avoid wave impacts (including diffraction and run-up effects from the pile), and ladders and fenders must be designed to withstand ship impacts.

The main focus of the present chapter is on global response analysis for OWTs, while detailed strength assessment is left to standards and textbooks (Clauss *et al*., 1982; NORSOK, 2007; ABS, 2013; DNV, 2013). Firstly, simplified criteria and analysis tools that may be employed in the early stages of design are examined in Section 4.5. Next, an overview of environmental load considerations for global analysis is given in Section 4.6, while short-term and long-term structural analysis is described in Section 4.7.

4.5 Conceptual Design

Preliminary support structure design of OWTs is often carried out using simplified modelling and analysis tools. Whether designing a novel concept or scaling an existing design for a new location or turbine, simple models are needed in order to determine whether or not the design satisfies basic criteria, such as static equilibrium, maximum offsets, maximum pitch angles and natural periods of rigid body motions for floating platforms, or mudline displacements and system natural periods for vibrations of bottom-fixed platforms. Decisions regarding the feasibility or direction of a project often depend on initial estimates of size, manufacturability or ease of installation, and cost.

4.5.1 Initial Design Criteria

While the final design of an OWT support structure requires consideration of numerous load cases, design criteria at the initial stage are often described in terms of more basic global characteristics, such as natural periods and offsets. These criteria should, of course, be rational and able to give a reasonable prediction of the structural integrity, functionality or of the system cost.

As an example, limits on the natural periods of the system as a whole are physically related to the system responses: in order to limit the resonant responses and corresponding load cycles (which may affect both ultimate and fatigue load effects), the natural periods should not coincide with the linear wave excitation or with important rotor frequencies. The critical rotor frequencies for the lowest structural modes are typically 1p (the rotor frequency) and *n*p (the blade passing frequency where *n* is the number of blades, which may be excited through tower shadow effects, and sampling of the sheared, yawed or turbulent inflow). The lowest natural frequency for a bottom-fixed wind turbine is typically a global bending mode; this frequency is often placed in between the 1p and *n*p frequencies (this can be described as a soft–stiff design).

Case study 4.1 – Natural frequency placement for a 5-MW bottom-fixed wind turbine

Consider the three-bladed, variable speed NREL 5-MW wind turbine (Jonkman *et al*., 2009), to be placed on a bottom-fixed support structure and tower in 20 m water depth. The support structure and tower are to be constructed from a single uniform steel cylinder, extending from the seabed (fully fixed) to the hub height (90 m above sea level). Assuming a diameter-to-thickness ratio of 80, the only design variable is the diameter of the cylinder (*D*). Based on this simplified system (Figure 4.4) and disregarding added mass, identify values of *D* which result in placement of the first natural frequency in between the 1p and 3p excitation frequencies.

Firstly, we can begin by identifying the limiting 1p and 3p frequencies. The 1p frequency varies from 6.9 rpm at cut-in to 12.1 rpm at rated speed (0.72 to 1.26 rad/s). The 3p frequency range is found by simply multiplying these values by 3, that is 2.16 to 3.78 rad/s. The limiting frequencies are thus 1.26 and 2.16 rad/s.

Then, we can estimate the first natural frequency of the simplified system as (Stokey, 1961):

$$\omega = \sqrt{k / \left(0.23 m_{beam} + M_{RNA}\right)}$$

The stiffness of the beam is $k = \frac{3EI}{L^3}$, where $I = \frac{\pi}{64}(D^4 - (D-2t)^4)$ for a circular cross-section. The beam mass is computed from the cross-sectional area as:

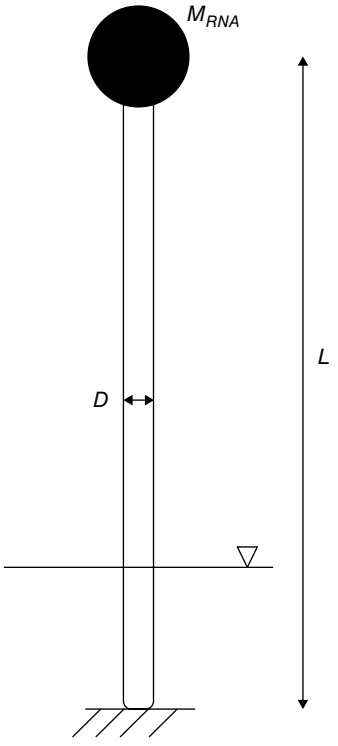

Figure 4.4 Simplified model of the bottom-fixed turbine.

$$m_{beam} = \frac{\rho\pi}{4}(D^2 - (D-2t)^2)$$

while the RNA mass is given in Table 4.1.

The resulting natural frequencies are compared to the wind turbine and wave excitation in Figure 4.5. Based on the wave environment, one would typically aim toward the higher end of this allowable range. Despite the simplifications in the analysis, the obtained diameter of roughly 5.5–6 m corresponds reasonably well with real designs for similar turbines. In reality, of course, the diameter and thickness would vary along the length, and other considerations such as buckling would be included.

Table 4.1 Case study parameters.

RNA mass (M_{RNA}) (tonnes)	350
Cut-in rotor speed (rpm)	6.9
Rated rotor speed (rpm)	12.1
L (m)	110
D/t	80
Density (ρ) (kg/m^3)	8000
Young's Modulus (E) (GPa)	210

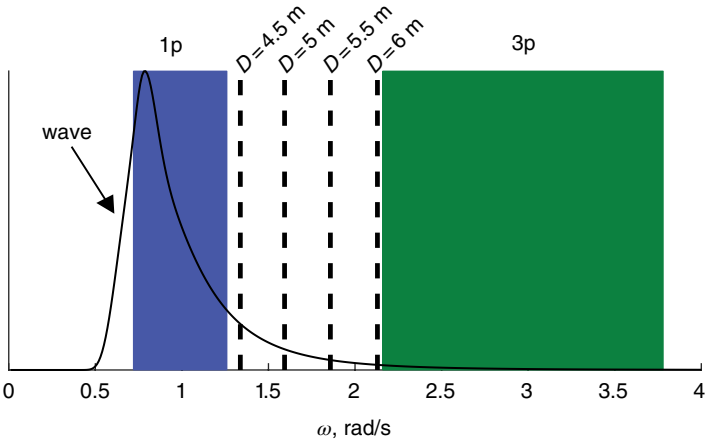

Figure 4.5 Obtained frequencies for variable diameter, compared to 1p and 3p ranges and typical wave spectrum.

For floating wind turbines, the placement of both rigid body motions and of the first tower bending modes should be considered. Natural frequencies of rigid body motions should be placed far below or far above the typical wave excitation frequencies (0.04–0.25 Hz). As such, resonant responses due to linear wave excitation can be avoided; nonlinear wave loading can still reach the natural frequency of such structures. Most catenary-moored floating systems are designed to have all of their natural frequencies of rigid body motions well below the wave excitation range, with the possible exception of yaw, which is not usually directly excited by linear wave actions. TLPs, on the other hand, typically have vertical modes of motion with natural frequencies far above the wave frequency. Equilibrium in the dynamic system implies that the linear wave excitation loads must be balanced by a combination of the inertial loads due to the platform motions, restoring forces (hydrostatic or in the mooring system) and damping. For catenary-moored structures, the linear wave loads induce platform motions while the tension in the mooring lines is small. For tautly-moored structures, high tendon or line tension counteracts linear wave loads and the corresponding platform motions are restricted or small.

Table 4.2 displays typical natural periods of rigid body motions for FWTs. Suggested typical values, as well as observed values from published studies of 5-MW FWTs, are shown. For comparison, the 1p period of the studied turbine ranges from 5 to 8.6 s (3p from 1.7 to 2.9 s). As shown, the spar concepts tend to be far from the wave excitation in surge, heave and pitch, while the yaw motion may approach wave (or 1p) frequencies. Semi-submersibles similarly tend to have periods well above the wave periods, although maintaining a long heave period can be a challenge. TLPs and TLBs both have short periods in heave and pitch, while TLPs have longer periods in surge and yaw. It should be noted that the pitch natural period of TLPs and TLBs is generally a flexible mode, tightly coupled to tower bending. As such, the method of estimation of the natural frequency may have a significant influence on the obtained result.

Table 4.2 Natural periods of rigid body motions of floating offshore wind turbines. Typical values from Chen and Yu (2013) are given in parenthesis, follow by observed values from published studies of 5-MW designs.

	Spar	**Semi-submersible**	**TLP**	**TLB**
Studies	Matha, 2009; Utsunomiya *et al.*, 2010; Myhr *et al.*, 2011	Roddier *et al.*, 2011; Goupee *et al.*, 2014; Koo *et al.*, 2014; Luan *et al.*, 2016	Matha, 2009; Henderson *et al.*, 2010; Suzuki *et al.*, 2010; Bae *et al.*, 2011; Bachynski and Moan, 2012; Zhao *et al.*, 2012	Myhr *et al.*, 2011
Surge/ sway (s)	(>40), 50–185	(>40), 80–117	(>40), 20–60	3–4
Heave (s)	(20–50), 27–30	(17–40), 17.5–25.8	(<5), 0.6–4.9	3–4
Pitch/ roll (s)	(25–60), 27–35	(25–50), 26–43	(<5), 0.92–4.5[a]	2–4
Yaw (s)	(>3), 8–38	(>3), 58–83	(>3), 10–27	8

[a] The pitch natural frequency for a TLP may not be well defined due to coupling with tower bending and elasticity in the floater itself. When accounting for the flexibility in the tower, the lowest natural period tends to be above 3.2 s.

For FWTs, the natural frequency of the first bending modes of the tower should be considered in addition to the rigid body motions (Kvittem *et al.*, 2011; Bachynski *et al.*, 2014). Compared to a cantilevered tower with the same length and the same top mass, the natural frequency of the first bending mode of the tower tends to increase when it is placed on a floating platform. The increase in natural frequency is related to the change in boundary conditions: the mass and stiffness of the floating platform must be taken into account, and the lowest frequency of rotation is no longer the first bending mode, but rather a rigid body displacement in pitch.

In addition to the limits on natural periods, other preliminary design criteria for OWTs are typically related to expected maximum responses in the at-rated (maximum thrust) or storm (maximum wave) conditions. For example, some typical assumed limits for monopile designs are expressed in terms of maximum lateral deflections (20 mm at the pile tow and 120 mm at the mudline) or maximum rotation at the mudline (0.25° without tolerance) (DNV, 2007; Krolis *et al.*, 2010). A 'zero toe-kick' criterion is often prescribed – requiring that the neutral line of the pile is vertical for at least one location under maximum load – but this is based on flexible pile behaviour and may not be appropriate for large diameter piles (which behave more like a rigid pile) (Krolis *et al.*, 2010).

For FWTs, the platform offsets in surge and pitch at the rated wind speed are often considered. Limitations on the maximum surge may be related to the anchors (for example, TLP anchors are often not designed for more than 10° angles at the seabed, or drag anchors may not be designed to take vertical loads) or to the allowable stresses in the electrical cable or mooring system (i.e. avoiding slack). Limitations on the allowable mean pitch angle of the platform may be related to limitations provided by the turbine manufacturer (typically dictated by the generator) or to an effort to keep the turbine approximately vertical in order to maximize power output. Of course, when applying criteria based on the mean thrust loads, an allowance for dynamic responses should be included.

4.5.2 Design by Upscaling

As wind turbines move farther offshore and the industry becomes more mature, turbine size is increasing. Although the mass of the rotor theoretically increases faster than the power rating, the benefits of a reduced number of turbines and support structures can reduce the costs of installation and maintenance. It is, therefore, interesting to consider the scaling laws that affect the rotor, tower, and support structure.

For rotor scaling, the primary consideration is the power rating. The power output (P) of a wind turbine can be defined as:

$$P = \frac{\pi}{2} \rho C_p R^2 u^3 \tag{4.4}$$

where ρ is the density of air, C_p is the power coefficient (with a theoretical maximum of 16/27), R is the rotor radius and u is the wind speed. As shown in Equation 4.4, assuming the same wind speed and power coefficient, power increases with the length scale ($\lambda = R_{upscaled}/R_{original}$) squared. Table 4.3 shows the theoretical change in various quantities based on the length scale for a wind turbine operating at the same tip-speed ratio in identical wind conditions. The real observed scale factors for these quantities differ

Table 4.3 Wind turbine upscaling based on length scale ratio, λ.

Quantity	Scale ratio
Power	λ^2
Rotational speed	λ^{-1}
Thrust/aerodynamic forces	λ^2
Torque/aerodynamic moments	λ^3
Mass	λ^3

from the theoretical values for numerous reasons, including: changes in technology (such as new aerofoils or materials), higher wind speeds (due to the increase in hub height or change of location) or changes in the control or operation of the turbine. Still, it is worthwhile to note that structural stresses due to aerodynamic or centrifugal forces remain constant, while the loads due to self-weight increase linearly with the length scale.

Assuming linear geometric scaling of the rotor and support structure, the elastic structural frequencies can also be shown to scale with λ^{-1}, that is, the structural frequencies are reduced by the same amount as the rotor frequency. A structure that is properly designed with respect to avoiding excitation of natural frequencies due to the rotor speed and its harmonics will also avoid aeroelastic resonance problems after upscaling. On the other hand, for an OWT, and especially for bottom-fixed structures, the reduction in structural natural frequencies can make the system more sensitive to wave loads. For FWTs, the natural frequencies of rigid body motions of the platform will tend to scale with $\lambda^{-1/2}$, such that catenary moored structures will move farther from the wave excitation, while tautly moored structures (with more 'elastic' modes) may require a greater degree of redesign. The exact scaling of the natural frequencies of horizontal rigid body motions of catenary moored structures also depends on the scaling of the mooring system.

4.5.3 Preliminary Analysis

To check that a conceptual design satisfies the criteria from Section 4.5.1, simple hand calculations are often employed. For bottom-fixed wind turbines, a simple beam element model with initial estimates of the soil stiffness may be sufficient for estimating natural frequencies. For a FWT, the geometry determines the buoyancy, while the dry mass, added mass and stiffness due to hydrostatics and the mooring system should be estimated in order to obtain a stable floating system with desired natural periods.

The dry mass of the FWT hull includes both the steel (or concrete) mass as well as ballast. Preliminary estimates of the structural mass per displaced volume may be obtained from existing platform designs. Selected values of the structural steel mass (considering only the hull, not the tower or turbine mass) divided by the displaced mass of FWT platforms are given in Table 4.4. The provided published values do not necessarily represent optimized designs: one would expect that a semi-submersible platform with braces should give a more steel-efficient design compared to a brace-less concept. The steel plate thickness for a spar tends to be dictated by local hydrostatic pressure, while dynamic loads may be governing for other concepts.

Table 4.4 Steel mass fraction for various steel FWT platforms.

Platform	Hull steel mass per displaced mass
Spar (Ormberg and Bachynski, 2015)	0.13
Brace-less semi-submersible (Luan *et al.*, 2016)	0.17
TLP (Bachynski and Moan, 2012)	0.22
Semi-submersible (OC4) (Robertson *et al.*, 2012)	0.27

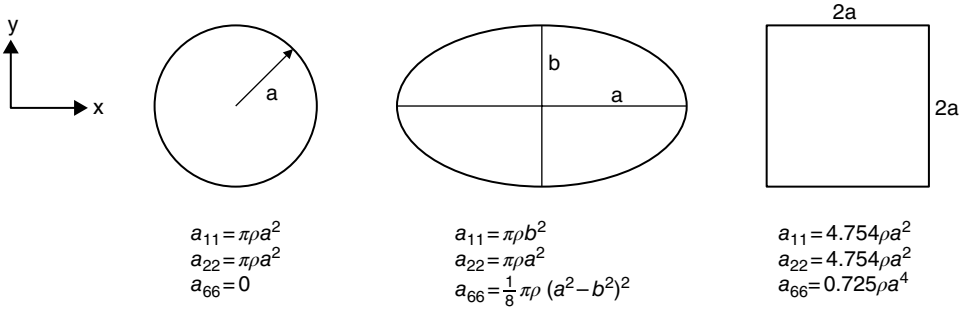

Figure 4.6 2-D added mass for simple shapes (Newman, 1977). The *x* direction is denoted 1, while *y* is 2, and rotation about the *z*-axis is 6.

In order to estimate the added mass without building a panel model and solving the potential flow problem, simple 2-D estimates may be combined using strip theory, such as those shown in Figure 4.6. Furthermore, the added mass in heave of a surface-piercing vertical circular column can be estimated as half of the displaced mass of a sphere with the same diameter (Chakrabarti and Hanna, 1990). The added mass of heave/pitch plates, which are commonly used to increase the added mass and damping of semi-submersibles, may require more detailed analysis (Roddier *et al.*, 2011).

The hydrostatic stiffness is relatively easy to estimate when the geometry and centre of gravity are known. An expression for the hydrostatic stiffness in pitch was given in Equation 4.1; the hydrostatic stiffness in heave is obtained simply from the waterplane area (A_{wp}) as in Equation 4.5:

$$C_{33} = \rho g A_{wp} \tag{4.5}$$

Finally, the mooring system stiffness may be estimated using quasi-static methods for a catenary system (Faltinsen, 1990) or by modelling the TLP tendons linearly (Jain, 1980; Bachynski, 2014). The obtained mooring system stiffness is important for estimating both natural periods and offsets.

Using these simple calculations, rigid-body natural frequencies of a FWT can then be obtained by solving for the nonzero combinations of frequency (ω) and the displacement vector ($\vec{x}$) that satisfy Equation 4.6:

$$\left(-\omega^2\left[\boldsymbol{M}+\boldsymbol{A}\right]+\left[\boldsymbol{C}+\boldsymbol{K}\right]\right)\vec{x} = 0 \tag{4.6}$$

Eigenvalue methods can be applied when the matrix $(\boldsymbol{M}+\boldsymbol{A})$ is symmetric and positive definite. Alternatively, simpler methods can be used, such as reducing the problem by neglecting couplings completely, or by considering only two coupled degrees of freedom at a time. In particular, the added mass coupling between surge and pitch may be important, while heave can often be considered independently.

Case study 4.2 – Estimation of the natural periods of the OC4 semi-submersible

Consider the OC4 semi-submersible wind turbine (Robertson *et al*., 2012, 2013b) shown in Figure 4.7, with dimensions as given in Table 4.5. Estimate the natural periods of rigid body motion using analytical approximations for the added mass with the provided coefficient C_a for horizontal motion, the given nonzero terms of the linearized mooring system stiffness matrix and approximations of the hydrostatic stiffness. Effects from the horizontal and diagonal braces may be ignored.

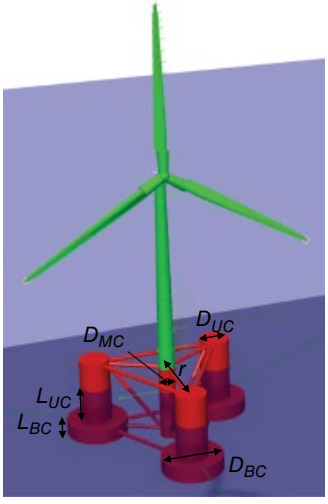

Figure 4.7 OC4 semi-submersible modelled in SIMA.

The added mass in surge can be estimated by strip theory, using the 2-D coefficient for a circular cylinder in Figure 4.6 and the given C_a, which accounts for some diffraction effects. The heave added mass (A_{33}) can be approximated as the sum of the corresponding 'half-sphere' for the centre column and twice the 'half-sphere' for each of the base columns minus the approximate volume of the upper column within the upper half-sphere. The pitch added mass (A_{55}) is integrated from the local surge and heave added mass, while the surge-pitch coupling (A_{51}) and yaw added mass (A_{66}) are approximated using only the surge coefficients.

Table 4.5 Case study parameters.

D_{MC} (m)	6.5	P (kg/m$^{3)}$	1025
D_{UC} (m)	12	M_{tot} (tonnes)	14073
D_{BC} (m)	24	M_{44}, M_{55} (tonnes-m^2)	1.26E + 07
L_{UC} (m)	14	M_{66} (tonnes-m^2)	1.26E + 07
L_{BC} (m)	6	V_0 (m^3)	13557
T (m)	20	K_{11}, K_{22} (N/m)	7.08E + 04
z_B (m)	−13.15	K_{33} (N/m)	1.91E + 04
z_G (m)	−9.88	K_{44}, K_{55} (Nm/red)	8.73E + 08
r (m)	28.9	K_{66} (Nm/rad)	1.17E + 08
C_a	0.6	K_{15}, $-K_{24}$, K_{51}, $-K_{42}$ (Nm/m)	−1.08E + 05

When assembling the added mass matrix, $A_{22} = A_{11}$, $A_{44} = A_{55}$, and $A_{42} = -A_{51}$, and the matrix is symmetric:

$$A_{11} \approx C_a \frac{\pi\rho}{4}\left(D_{MC}^2 T + 3D_{UC}^2 L_{UC} + 3D_{BC}^2 L_{BC}\right) \qquad A_{51} \approx -\frac{3C_a\rho\pi}{8}\left(L_{UC}^2 D_{UC}^2 + (T^2 - (L_{BC} - T)^2)D_{BC}^2\right)$$

$$A_{33} \approx \rho\pi\left(\frac{D_{MC}^3}{12} + \frac{D_{BC}^3}{2} - \frac{D_{BC}D_{UC}^2}{2}\right) \qquad A_{66} \approx \frac{3C_a\rho\pi}{4}\left(L_{UC}D_{UC}^2 + L_{BC}D_{BC}^2\right)r^2$$

$$A_{55} \approx \frac{3C_a\rho\pi}{4}\left[D_{UC}^2 L_{UC}\left(\frac{L_{UC}^2}{12} + \frac{L_{UC}^2}{4}\right) + D_{BC}^2 L_{BC}\left(\frac{L_{BC}^2}{12} + \frac{\left(-2T + L_{BC}\right)^2}{4}\right)\right] + \frac{\rho}{2}D_{BC}^3 r^2$$

The hydrostatic stiffness coefficients are obtained from Equations 4.5 and 4.1. The eigenvalue problem in Equation 4.6 can then be formed (as below, in tonnes and kN) and solved, or the decoupled motions can be examined using only the diagonal terms. The results of the coupled and decoupled simplified method are compared to results from time domain simulations of the complete finite element model in MARINTEK's SIMA software (including correct added mass) in Figure 4.8.

$$\left(-\omega^2\left(\begin{bmatrix} 1.41E4 & 0 & 0 & 0 & -1.39E5 & 0 \\ 0 & 1.41E4 & 0 & 1.39E5 & 0 & 0 \\ 0 & 0 & 1.41E4 & 0 & 0 & 0 \\ 0 & 1.39E5 & 0 & 1.26E7 & 0 & 0 \\ -1.39E5 & 0 & 0 & 0 & 1.26E7 & 0 \\ 0 & 0 & 0 & 0 & 0 & 1.23E7 \end{bmatrix} + \begin{bmatrix} 8.33E3 & 0 & 0 & 0 & -1.06E5 & 0 \\ 0 & 8.33E3 & 0 & 1.06E5 & 0 & 0 \\ 0 & 0 & 1.67E4 & 0 & 0 & 0 \\ 0 & 1.06E5 & 0 & 7.55E6 & 0 & 0 \\ -1.06E5 & 0 & 0 & 0 & 7.55E6 & 0 \\ 0 & 0 & 0 & 0 & 0 & 6.61E6 \end{bmatrix}\right) + \left(\begin{bmatrix} 0 & 0 & 0 & 0 & 0 & 0 \\ 0 & 0 & 0 & 0 & 0 & 0 \\ 0 & 0 & 3.74E3 & 0 & 0 & 0 \\ 0 & 0 & 0 & 1.03E6 & 0 & 0 \\ 0 & 0 & 0 & 0 & 1.03E6 & 0 \\ 0 & 0 & 0 & 0 & 0 & 0 \end{bmatrix} + \begin{bmatrix} 70.8 & 0 & 0 & 0 & -108 & 0 \\ 0 & 70.8 & 0 & 108 & 0 & 0 \\ 0 & 0 & 19.1 & 0 & 0 & 0 \\ 0 & 108 & 0 & 8.73E4 & 0 & 0 \\ -108 & 0 & 0 & 0 & 8.73E4 & 0 \\ 0 & 0 & 0 & 0 & 0 & 1.17E5 \end{bmatrix}\right)\right) x = 0$$

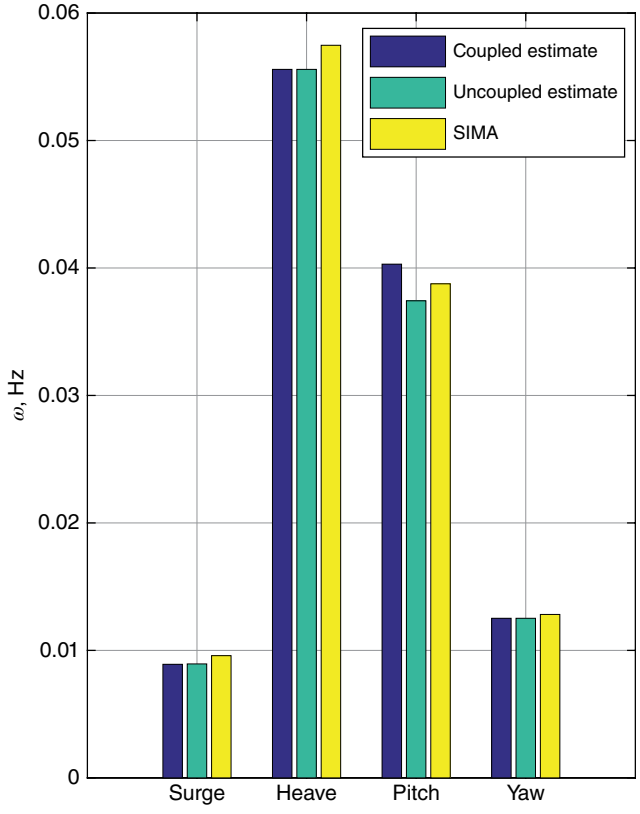

Figure 4.8 Obtained estimates of the natural frequencies of the OC4 semi-submersible.

To improve the design at an early stage, parametric modelling of the hull – that is, defining the hull as a combination of simple geometrical shapes and defining their dimensions as parameters – can be combined with these simplified analytical models. An early optimization of the design can then be made possible by including a cost model (Crozier, 2011; Fylling and Berthelsen, 2011; Bachynski, 2014). The cost model might include the steel mass, dimensions, mooring system dimensions and loads. For a spar buoy, Fylling and Berthelsen (2011) showed an 18 % cost reduction through preliminary optimization, considering platform response in extreme conditions and mooring system fatigue.

4.6 Loads in the Marine Environment

Complex, challenging, quasi-static and dynamic environmental conditions characterize the marine environment with which OWT support structures interact. Even on a perfectly calm day, tidal variations can modify the static equilibrium of a tautly-moored structure or generate strong currents. Offshore sites are inherently chosen to have a good wind resource, which also implies significant dynamic loads from wind and waves, in addition to current- and possible ice-induced loads. A brief introduction to the relevant topics in aerodynamics and hydrodynamics is given here, with references to more detailed textbooks on these extensive subjects.

4.6.1 Aerodynamic Loads

Wind-induced loads are often design-driving for OWT support structures, although the relative importance of wave loads tends to increase as water depth increases. When considering the support structure design for a given location, the variations in the wind in time and space may be important: temporal variations are characterized as seasonal, diurnal and short term (turbulence and gusts), while important local spatial variations include the shear effect of the boundary layer and wake effects from neighbouring wind turbines. The wind resource is discussed in greater detail in various textbooks (Manwell *et al*, 2009; Burton *et al*., 2011).

The wind turbine rotor and tower, as well as any components of the support structure that are above the wave surface, are directly affected by the incoming turbulent wind. The aerodynamic loads from the rotor are most significant in typical operational conditions, but drag forces on the tower and support structure (typically assumed proportional to the wind velocity squared) may become significant in extreme conditions when the rotor is parked. For example, consider a 5-MW wind turbine with tower of length $L = 90$ m, average tower diameter $D = 5$ m, and maximum thrust load at rated wind speed of 700 kN (Jonkman *et al*., 2009). In an extreme wind speed $u_w = 35$ m/s (assumed averaged over the tower), the load on the tower can be estimated as:

$$F = \frac{1}{2} C_D \rho_{air} u_w^2 DL \tag{4.7}$$

which suggests a load of approximately 340 kN (taking $\rho_{air} = 1.225\,\text{kg/m}^3$ and $C_D = 1$), which could be larger than the corresponding rotor load for a parked turbine.

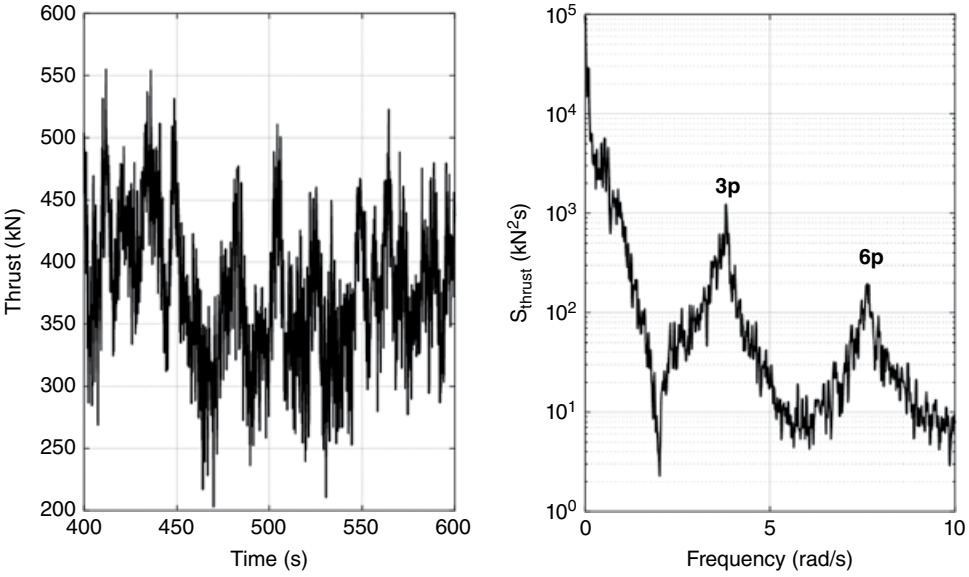

Figure 4.9 (Partial) time series and spectrum of thrust force from bottom-fixed NREL 5-MW OWT in turbulent wind, 15 m/s.

Aerodynamic models for wind turbines range from one-dimensional (1-D) momentum balance models to full 3-D Navier–Stokes solutions. Blade element momentum (BEM) and generalized dynamic wake (GDW) models are computationally efficient tools that can easily be coupled to beam element structural models. The BEM method is based on the conservation of momentum and mass, and the requirement that local lift and drag forces at the aerofoils be consistent with the momentum equation. Although the method is based on constant wind and the assumption of an infinite number of blades, engineering corrections such as Glauert's correction for high induction factors, Prandtl's correction for tip and hub losses, dynamic stall corrections, dynamic wake corrections and tower influence modifications have been developed, and the application has been extended to dynamic conditions (Manwell *et al*., 2009; Burton *et al*., 2011). Despite the limitations of BEM and GDW, such as their inability to account for large rotor cone or large blade deflections, such methods give fairly accurate results for many operational conditions (Hansen *et al*., 2006).

The magnitude and frequency content of the loads induced by the rotor are critical for the support structure design. The rotor loads are closely linked to the incoming wind and to the control system actions. Figure 4.9 shows an example of the thrust force from a bottom-fixed wind turbine, in the time domain and the frequency domain. Note that the frequency domain results are shown with a log scale *y*-axis. As shown, the thrust force has a significant low frequency component, and the harmonics of the rotor speed are clearly visible. The low frequency component can be important for the excitation of natural periods of catenary moored structures and of TLPs in surge. The harmonics of the rotor speed (especially 3p effects from the tower shadow, shaft tilt, wind shear, turbine yaw and turbulence sampling) can be critical for excitation of the lowest modes of bottom-fixed structures or tower modes. Since the thrust force

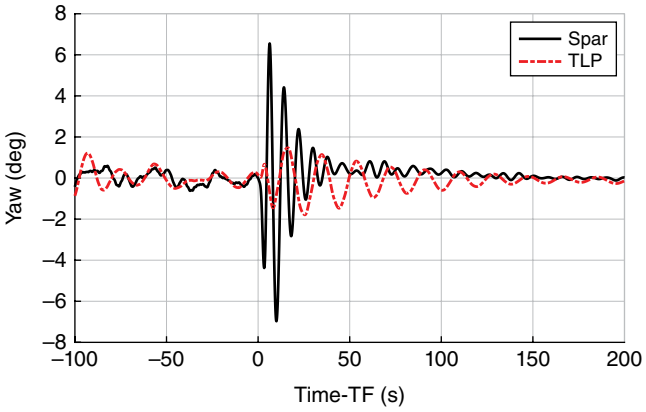

Figure 4.10 Yaw response of 5-MW spar and TLP FWTs induced by a combined blade pitch fault and shutdown at $t = 0$, rated wind speed and corresponding long-crested waves. (*Source:* Data from Bachynski *et al*., 2013.)

depends on the relative wind speed, an equivalent thrust spectrum for a floating wind turbine would show additional peaks at the wave frequency and natural frequencies in pitch and surge.

The coupling between the aerodynamic loads and structural motions is a particularly important effect that must be captured in OWT analysis. The rotor is exposed to the relative wind speed, which accounts for its own motion compared to the motion of the surrounding air: if the rotor moves toward the wind, the relative speed is higher. In general, this principle results in an aerodynamic damping effect. For bottom-fixed wind turbines, aerodynamic damping may be the dominant damping source in operational conditions. In above-rated wind speed conditions, however, depending on the frequency at which the control system responds and the structural natural frequency, negative feedback can occur. Control system effects may induce negative damping for FWTs, which requires modification to the control logic (Larsen and Hanson, 2007). Matha (2009) observed that it was possible to induce a surge instability for a TLP in a contrived condition, but the surge hydrodynamic damping is generally large enough to avoid unstable response. Flutter, aerodynamic effects and aerodynamic coupling to the floater motions must all be considered carefully with respect to stability.

Fault conditions may also induce aerodynamic loads that can have severe consequences for OWT support structures. As an example, a situation may be considered where the pitching mechanism for one of the blades stops working – perhaps due to a problem in the hydraulics – while the turbine is operating at above-rated wind speeds. There will be a resulting imbalance load in the turbine. If the supervisory control system detects the fault, a shutdown procedure (with two working blades) may be initiated. The shutdown procedure may induce a large negative thrust force as the blades pitch, which can in turn induce a significant transient response in the support structure (Bachynski *et al*., 2013; Jiang *et al*., 2013). As an example, the transient platform yaw responses of two FWTs during two-bladed shutdown are illustrated in Figure 4.10.

4.6.2 Hydrodynamic Loads

The wetted components of OWTs are subjected to hydrostatic-, wave- and current-induced loads. The relative importance of these loads is highly design-dependent: hydrostatic loads may determine the plate thickness of some FWT hull regions, while steep and breaking wave loads may be design-driving for monopiles or for other parts of the FWT hull.

Hydrostatic loads can be calculated directly based on the geometry and water characteristics. In a coordinate system with the still water level at $z = 0$ and the z-axis oriented upward, the hydrostatic pressure is $p = -\rho g z$, where ρ is the water density (typically 1025 kg/m^3 for salt water) and g is the acceleration due to gravity. For a spar platform with a draft of 100 m, the keel is then subjected to approximately 1000 kPa external pressure, which is a significant load. Of course, the lowest sections of a spar may be filled with ballast that counteracts some of this pressure. In addition to these hydrostatic loads, the support structure must withstand hydrodynamic pressure from waves and current.

The ocean waves that are of interest for OWT support structures are primarily generated by wind, either locally (called wind-waves, with periods around 5–15 s) or at a different location (typically called swell-waves, characterized by longer periods and a narrower frequency band) (Neumann and Pierson, 1966). The waves are stochastic and irregular. A simple model of the sea surface in a short-term period of, for example, three hours, is a combination of linear harmonic waves with different frequencies, phases, and directions. For example, the elevation could be given as:

$$\zeta = \sum_{j=1}^{N}\sum_{m=1}^{M}\sqrt{\left(2S\left(\omega_j,\theta_m\right)\Delta\omega_j\Delta\theta_m\right)}\sin\left(\omega_j t - k_j x\cos\left(\theta_m\right) - k_j y\sin\left(\theta_m\right) + \varepsilon_{jm}\right) \quad (4.8)$$

where ω represents the wave frequency, θ is the wave direction, ϵ is the phase and k is the wave number (Faltinsen, 1990). The wave number and frequency are related through a dispersion relation, which depends on water depth. As shown in Equation 4.8, the amplitude of each component is a function of the joint wave amplitude and direction spectrum, S. The wave spectrum provides a description of the short-term sea state: that is, the wave spectrum is used to describe the statistical properties of the wave over a time period where certain characteristic values (typically significant wave height, H_s, and peak period, T_p) can be considered constant. For OWT analysis, the spectral description of the waves should be chosen carefully to correctly represent the frequency distribution of local conditions, including both wind sea and swell sea, as well as their respective spreading. Note that a variety of short term conditions must be considered in the evaluation of an OWT (Section 4.7) and that second order models for the wave loads may be necessary (NORSOK, 2007).

This simplified description of the sea surface is useful for the development of wave load models, as the linear harmonic wave elevation can be related to the solution of the Laplace equation with appropriate boundary conditions. The obtained velocity potential gives explicit expressions for velocities and accelerations in the wave field. Considering a single component of the wave elevation from Equation 4.8, travelling in the x-direction with frequency ω_j, the horizontal velocity (u_j) and acceleration (a_j) are given by:

$$u_j = \omega_j \zeta_j \sin\left(\omega_j t - k_j x\right)\frac{\cosh k_j\left(z+h\right)}{\sinh\left(k_j h\right)} \quad (4.9)$$

$$a_j = \omega_j^2 \zeta_j \cos\left(\omega_j t - k_j x\right) \frac{\cosh k_j \left(z+h\right)}{\sinh\left(k_j h\right)} \tag{4.10}$$

where ζ_j is the amplitude of the wave component, h is the water depth and z is the vertical coordinate (0 at the mean free surface, positive upward).

For relatively small or slender structures – which can be assumed to have little effect on the wave field – the hydrodynamic pressure loads can be estimated from the resulting undisturbed potential flow. For large volume structures, the velocity potential should be solved including the presence of the body, thereby including diffraction effects. Due to motions of the structure, additional consideration should be given to radiation loads, which can be described as added mass and linear damping in the frequency domain.

Morison's equation is often used to model the wave loads on slender cylindrical structures. The assumption of slenderness is taken to be reasonable for $\lambda > 5D$, where λ is the wavelength and D is the structural diameter. A formulation for the horizontal force (dF) on a vertical strip of length dz of a vertical cylinder, including the effect of structural motion, is given in Equation 4.11:

$$dF = dz\left[\rho\pi\frac{D^2}{4}C_M a_1 - \rho\pi\left(C_M - 1\right)\frac{D^2}{4}\ddot{\eta}_1 + \frac{1}{2}C_D D\left(u - \dot{\eta}_1\right)\left|u - \dot{\eta}_1\right|\right] \tag{4.11}$$

In Equation 4.11, the first two terms are related to the added mass and Froude–Krylov excitation forces, and depend on the mass coefficient (C_M), wave particle horizontal acceleration (a_1) and horizontal acceleration of the strip ($\ddot{\eta}_1$). Based on potential flow, for a circular cylinder in the long wave limit, $C_M = 2$, where half of the contribution comes from the Froude–Krylov excitation and half from diffraction. The added mass is related to the fluid pressure caused by the acceleration of the structure, and a coefficient $C_a = C_M - 1$ can be defined. The last term accounts for viscous drag forces and depends on the drag coefficient (C_D), wave particle horizontal velocity (u) and horizontal velocity of the strip ($\dot{\eta}_1$). Although there are limitations to its applicability, this semi-empirical equation can capture some of the important physically observed wave load characteristics:

- The importance of the inertia terms compared to the drag term depends on the wave height to diameter ratio (H/D), with drag becoming more important as H/D increases.
- The inertia loads act with the same frequency as the waves themselves and are concentrated in regions with high wave particle accelerations (i.e. near the free surface).
- Drag effects include a higher frequency contribution (at three times the wave frequency) due to the velocity squared term. This loading can be particularly important for bottom-fixed wind turbines. Viscous drag effects also contribute damping due to the use of the relative velocity.

The wave loads discussed so far – using first order potential flow models or Morison's equation with linear wave kinematics – are primarily linear (except for the quadratic drag term). In reality, there are nonlinearities in the wave loads that are important for modelling OWTs.

For bottom-fixed wind turbines, the effects of nonlinear waves (including breaking waves) and nonlinear diffraction may be important. The nonlinearity of shallow water waves, particularly in storm conditions, can become significant, such that linear

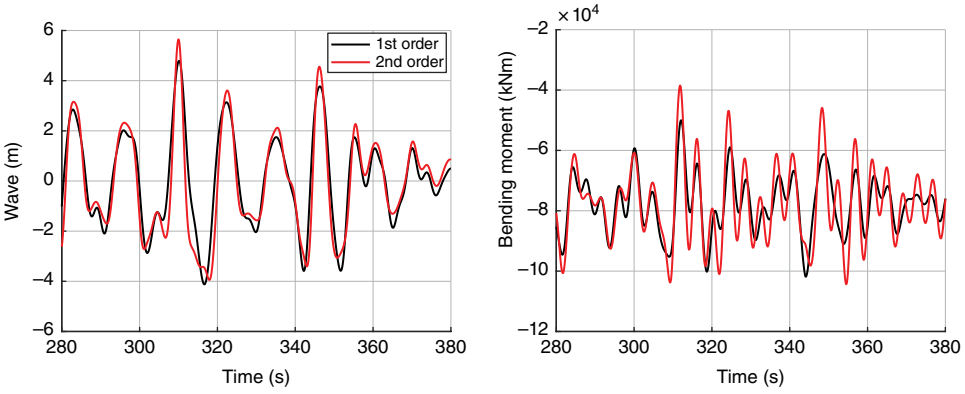

Figure 4.11 Example of wave elevation (left) and load effects (bending moment in the monopile near the free surface), comparing first and second order waves in 20 m water depth, H_s 6.5 m, T_p 13 s. Simulations in SIMA software (MARINTEK).

modelling of the kinematics is not sufficient. The high frequency loads related to steep, nonlinear waves may be able to excite *springing* (steady state) or *ringing* (transient) responses of OWTs (Zang *et al*., 2010). Furthermore, breaking waves can impart significant loads: correct physical modelling of these loads is an area of active research (Wienke and Oumeraci, 2005; de Ridder *et al*., 2011; Bredmose *et al*., 2013).

Figure 4.11 illustrates the difference between a second order irregular wave kinematics model and a first order model. The wave elevation for a severe sea state in shallow water is shown, as well as the corresponding internal bending moment in the wind turbine. Constant wind and a parked turbine are applied here. As shown, the wave crests are higher, and the troughs shallower, when the second order corrections are included. The increased high frequency loading can be seen in the amplitude of the vibrations of the structure at the first natural period. It should, however, be noted that the simulated sea state would, in reality, also include breaking waves, which are not modelled here. Wave breaking induces dissipation of energy, such that a lower significant wave height might be expected in reality, as well as higher loads of typically shorter duration than those induced by nonbreaking waves.

Nonlinear wave loads can also be important for floating structures. Second order wave loads include components at sum- and difference-frequencies of the primary wave frequencies. Sum-frequency effects and ringing loads have been shown to have significant consequences on fatigue and ultimate loads for TLPs, which have short natural periods in heave and pitch (Roald *et al*., 2013; Bachynski and Moan, 2014a, 2014b). Bachynski and Moan (2014a) showed that second order loads could cause 5–30 % increases in the standard deviation of key parameters such as pitch motions, tendon tension and tower base bending moments for TLP FWTs in extreme conditions; ringing loads were associated with increases in the maximum loads of 5–40 %. Slowly varying wave forces on catenary moored structures may also have impacts on maximum offsets and mooring loads (Coulling *et al*., 2013).

Hydrodynamic loads are, however, not only related to wave effects. Ocean currents – driven by wind, tides, geostrophic effects – are also important to consider. Not only can currents contribute static and slowly-varying loads, but interaction with the waves may

also result in modification of the frequency and magnitude of wave-induced loads. Furthermore, the potential for vortex-induced vibrations or vortex-induced motions should be considered.

While the present treatment of hydrodynamic loads should be considered as a cursory, descriptive introduction, more complete examinations of these topics can be found in textbooks (Newman, 1977; Faltinsen, 1990), and existing design standards may give practical guidance (DNV, 2007, 2010a, 2013; ABS 2013).

4.6.3 Additional Marine Loads

Placing wind turbines in the marine environment requires consideration of other factors in addition to the wind, waves, currents and hydrostatic pressure. Water level variations, ice, marine growth, seismic loads and soil–structure interactions should be accounted for in the design. In addition to these loads, which are discussed here, accidental loads (such as those from ship collisions) should also be accounted for.

Tides, driven by the gravitational pull between the Earth, Sun and Moon, result in variations in the mean sea level, with peaks occurring roughly twice each day. The magnitude of tidal variations is a complex problem and is also site specific, depending significantly on the local bathymetry (Neumann and Pierson, 1966). For smaller bodies of water, such as the Great Lakes, tidal variations may be less significant (less than 5 cm), but seiches – standing waves that are generated by weather conditions – can cause similar variations in mean water level over periods of several hours. Mean water level variations have real consequences for design: for bottom-fixed structures, the height of access platforms may depend on extreme tidal levels; installation procedures may be easiest to carry out for certain tidal conditions (or tidal current conditions); for TLPs, the mean tendon tension is also dependent on the water level. Additional temporary variations in water levels can occur due to storm surges, when water piles up against the coast (Neumann and Pierson, 1966). The combination of high tide and storm surge can cause a significant increase in the moment arm of wave forces acting on bottom-fixed support structures in extreme weather conditions.

In cold weather regions, offshore wind turbine support structure design should also account for ice and icing. Icing on the turbine and support structure can cause increases in gravitational and inertial loads, and icing on the blades modifies their aerodynamic performance, with possible consequences for the aerodynamic loading (Etemaddar *et al*., 2014). Sea ice can cause direct loads on the support structure, and dynamic interaction with the breaking ice around a support structure can excite structural natural frequencies. Compared to wind-only loads, increases of 60% in the maximum force and 10% in the bending moment were estimated for large wind turbines in Denmark (Gravesen *et al.*, 2005). Figure 4.12 compares the shear force at the mean water line for a monopile OWT under various load conditions as simulated by Shi *et al*. (2016). Fully coupled simulations are shown to have lower standard deviation than the superposition of responses under ice-only and wind-only loads (labelled as 'uncoupled').

Furthermore, in both fresh and saltwater environments, offshore structures are susceptible to marine growth or biofouling, as plants and animals attach themselves to surfaces underwater and in the splash zone. Marine growth can directly affect the structure's weight, geometry, and surface roughness. These effects can further modify the

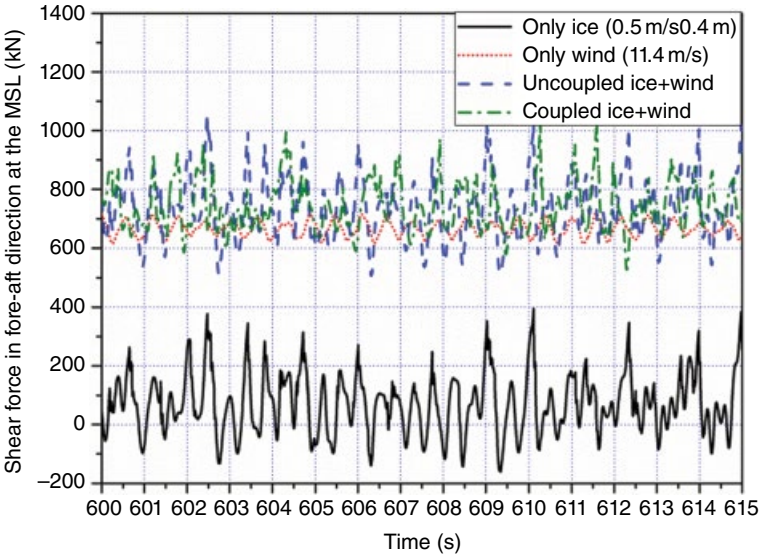

Figure 4.12 Comparison of the shear force in fore–aft direction at the mean sea level (MSL) under various load conditions. Ice thickness 0.4 m, ice drifting speed = 0.5 m/s, U_w 11.4 m/s, waterline diameter 8 m (*Source:* Shi *et al*., 2016. Reproduced with permission of Elsevier.).

hydrodynamic loads (for example, by increasing the diameter and modifying the drag coefficient C_D) and dynamic response, accessibility, and even the corrosion rate (DNV, 2007).

Finally, some portion of the support structure will necessarily be in direct contact with the seabed and the underlying soil. For piled foundations, soil–structure interaction is of particular importance for the determination of structural natural frequencies and the distribution of internal loads. Vertical loads are primarily taken up by friction in the soil, while overturning moments for monopiles are taken up by horizontal soil reactions. Local characteristics of the soil – such as the bearing capacity and friction – may require *in situ* measurements (Twidell and Gaudiosi, 2009). The direct contact with the soil can also lead to the transfer of seismic loads to the structure. These loads should, of course, be considered in design; however, Prowell and Veers (2009) suggest that, as turbine size increases, the seismic bending moment increases (scales) less quickly than the wind-induced moment.

4.7 Global Dynamic Analysis of Offshore Wind Turbines

Assessment of the responses of an OWT support structure requires consideration of extensive load cases to account for combinations of the wind and wave conditions, as well as various wind turbine operational or fault conditions, and possibly other loads. As described in the previous section, the loads and dynamics of the support structure are closely linked to the wind turbine. Global analysis is, therefore, considered necessary for support structure design; a global analysis using simplified models may also be combined with higher resolution local or decoupled analyses in order to examine the

strength of joints or dynamics of the wind turbine generator. A combination of numerical and experimental methods may be used for design of OWT support structures.

In the present sections, global analysis methods that can be used to estimate the load effects for power estimation and evaluation of design criteria (such as FLS or ULS) are discussed. Dynamic analysis models should include the mass and added mass, damping, stiffness and excitation of the important system components. Various levels of refinement can be considered in the model: for example, flexibility in the blades, tower, foundation and soil is expected to be important in the analysis of bottom-fixed OWTs, while rigid body models may be sufficient for estimating the motions of FWTs.

4.7.1 Short-term Numerical Global Analysis

To begin, consider how to evaluate the loads on an OWT support structure in a given stationary combined wind–wave–current condition. The short-term environmental conditions are typically defined in terms of H_s, T_p (Section 4.6.2), wave direction and other wave spectrum parameters, a mean wind speed (U_w), direction and turbulence intensity, as well as a wind spectrum or turbulence modelling parameters, and a current speed, direction and depth profile. The short-term conditions are exemplified in Figure 4.13. H_s is defined as the mean height of the 1/3 highest waves, while T_p corresponds to the frequency where the spectrum has its peak. The breadth of the wave spectrum may be additionally defined through a peak parameter, or it may follow naturally from the mathematical model of the spectrum. For the wind, the turbulence intensity is defined as the standard deviation of the wind speed divided by the mean wind speed. The time domain realization of irregular waves is carried out using an inverse fast Fourier transform (IFFT) based on the spectrum, and the turbulent wind time history can be generated by statistical (Jonkman, 2009) or physics-based models (Mann, 1998). The long-term environmental conditions are formulated as a site-specific joint probability distribution of the given parameters.

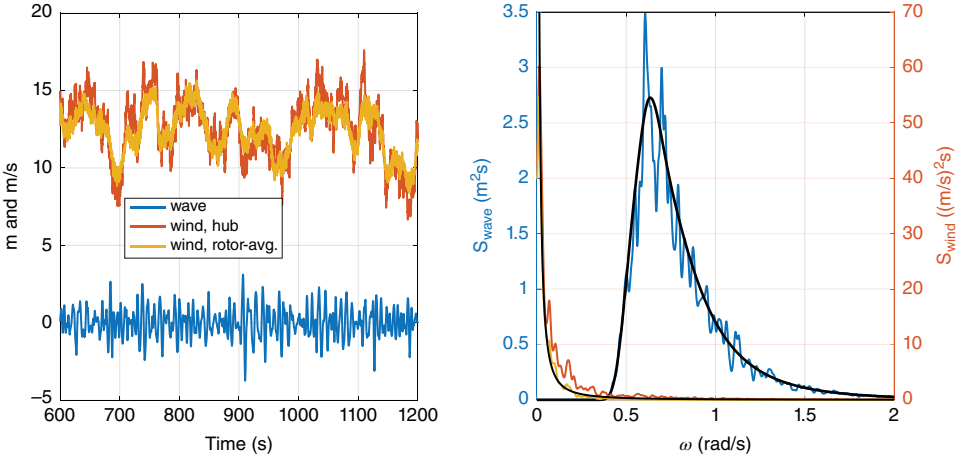

Figure 4.13 Time domain realization (left) and spectra (right) of a short-term wind and wave condition. Black curves show theoretical values of the spectra.

To carry out the short-term numerical analysis, one of the first choices is between frequency domain and time domain analyses. The frequency domain approach, which has been used extensively in the offshore industry, is computationally very efficient but normally requires linearization of the loads and responding structure. Time domain analyses allow for the inclusion of nonlinearity in the external loading, damping, geometrical or material stiffness, or boundary conditions. The actions of the wind turbine blade pitch and generator torque controller can thus be included, as well as quadratic damping, nonlinear wave loads, large deflections of the blades and large platform motions. Due to these advantages, time domain analyses are often preferred.

Nonetheless, due to the high computational cost of coupled time domain analyses, significant attention has been paid to the application of frequency domain methods for OWTs (van der Tempel, 2006). Kvittem and Moan (2015) presented a linear frequency domain (FD) approach for floating wind turbines. The method deals with the load effects in a rigid floating structure, exemplified with a semi-submersible wind turbine, and, especially, the flexural response in the tower, also considering structural dynamics effects. Aerodynamic damping from the rotor and hydrodynamic damping were included in calculations of the wave motions by applying a simplified formulation for the appropriate wind speed and a linearized form of Morison's equation, respectively. The load effect time histories from the wind-only and wave-only FD solutions were summed to find the total load effect histories. Relevant motion and stress load effects were found to deviate less than 15 % from the time domain simulation. The percentage error in fatigue damage estimates is about 3–5 times larger than uncertainties in the stress level, since fatigue damage is proportional to stress to the power 3–5.

The dynamic system may be discretized into a number of elements and the governing equation can be formulated by requiring that the virtual work done by externally applied loads be equal to the sum of the virtual work done by inertial, dissipative and internal forces. In a finite element (FE) analysis with a nodal displacement vector D, mass and damping matrices M_g and B_g, respectively, the global equation takes the form of:

$$M_g \ddot{\vec{D}} + B_g \dot{\vec{D}} + R_{int} = R_{ext} \tag{4.12}$$

where the internal reaction forces (R_{int}) are typically written as the product of a stiffness matrix and the displacement vector, and the external forces (R_{ext}) include the hydrodynamic and aerodynamic loads. Equation 4.12 is a system of coupled second order, spatially discretized, temporally continuous differential equations. The formulation of the mass, damping and stiffness matrices, and of the load and displacement vectors, depends on the type of elements to be used (Cook *et al.*; 2002; Hibbeler; 2005).

A common choice for OWT analysis is a combination of beam (tower, jacket, monopile, blades), bar (catenary mooring lines) and rigid elements (hull, hub, nacelle). Alternatively, a beam (or shell or solid) element model may be used to extract the most important mode shapes of the system, and the displacement vector may be formulated in terms of superposition of the selected mode shapes. For jacket OWTs, superelements may also be formulated for global analysis. The choice of elements represents a trade-off between fidelity and efficiency: it is, of course, feasible to discretize the system with a higher resolution – using, for example, shell or solid elements – but the analysis of numerous short-term conditions would be prohibitively computationally expensive. A modal analysis approach can significantly reduce computational demands

while still allowing for nonlinearities in the external loads. The material and geometric stiffness matrices are, however, linearized for modal analysis. If an accurate preprocessing is applied, modal analysis can be an accurate tool for OWT analysis; but the results are limited to the modes that are identified and included. The selection of the structural model is also related to how the aerodynamic or hydrodynamic loads are applied: rigid body models only allow for integrated forces and moments, while beam models allow for distributed line loads, and shell or solid models allow for distributed pressure loads.

Figure 4.14 illustrates one modelling approach for a global analysis of a TLP FWT. The structural model, which is representative of typical state-of-the-art global analysis, applies beam elements for most components, except for the hull; it uses BEM for the wind turbine aerodynamics and a combination of potential and Morison-type viscous loads for the hull. The active modes are illustrated based on filtered time domain results for the tower and tendons during a pitch decay test. The first mode of the tower bending is coupled with the first translational mode of the tendons, while the second tower bending mode is linked to the fourth tendon mode. If a modal analysis were to be considered, the higher modes of the tendons should therefore be included. The example does not include any flexibility in the hull, such that internal loads in general cannot be directly examined, although some models of spar wind turbines may combine Morison-type wave loads with flexible hull models (Karimirad and Moan, 2011). Novel methods to extract internal loads are also under development (Borg *et al,* 2016; Luan *et al.*, 2016).

The timescales of the physical problem are an important consideration for short-term time domain analysis of the system. These timescales affect the spatial discretization (or mode shapes for modal analysis) as well as the time step and simulation duration. Bottom-fixed offshore wind turbines have their longest natural periods around four seconds, while FWTs may have natural periods on the order of hundreds of seconds. The first natural periods of the blades (and, if appropriate, the first bending or torsional modes of floating platforms) should be resolved sufficiently. For FWTs, the longer periods of rigid body motion should also be included. On the load side, both slowly-varying wind and second-order wave loads as well as wave-frequency loads, 1p and 3p excitation, and, in some cases, sum-frequency wave loads must be captured. Consideration of the drivetrain typically requires even higher frequencies, such that drivetrain analysis is often carried out in a decoupled manner. Small time steps are needed to resolve the structural natural periods and load processes, while a sufficiently long duration is needed in order to reduce the statistical uncertainty of the short-term conditions.

The required – and appropriate – duration of short-term analyses is still an active research topic. The assumption of stationary wave conditions is often taken to be three hours in the offshore industry, while 10 minutes are typically assumed for wind in the wind industry. For floating structures, a 10-minute simulation is clearly too short to capture a sufficient number of cycles; three-hour calculations may require stretching the limits of the assumptions regarding stationarity of the wind. A large number of shorter conditions may be considered as an alternative but the results of such analyses must be evaluated properly, especially for extreme value analysis. For fatigue analysis, the required duration of analyses also depends to some extent on the number of conditions to be tested: if the long-term parameter space is discretized more finely, it may be possible to use shorter analysis duration for each condition and maintain the same

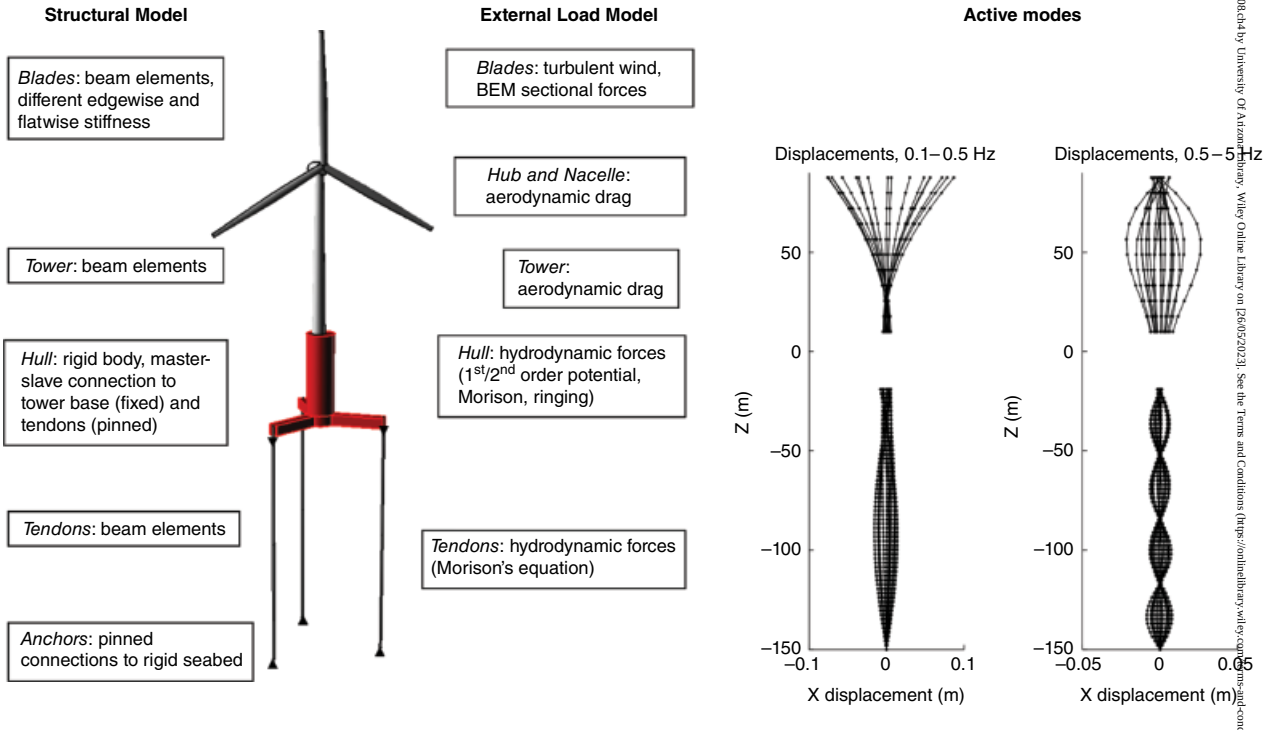

Figure 4.14 Example of global FE model strategy for a TLP FWT: structural model, external load models and active mode shapes in the tendons and tower (from pitch decay tests). (*Source:* Adapted from Bachynski, 2014.)

accuracy in fatigue calculations. Extreme value calculations are, however, more sensitive. When time domain simulations are being carried out, statistical uncertainty due to the limited number of realizations should also be considered.

4.7.2 Long-term Numerical Global Analysis

A variety of short-term numerical analyses described in the previous section must be carried out and combined correctly in order to determine the effects due to environmental loads, considering both extreme load effects (ULS design check) and load effect time histories (FLS design check) (Naess and Moan, 2013). A full long-term analysis (FLTA), in which all of the relevant environmental conditions and their probability of occurrence are taken into account, is considered the most accurate approach.

For extreme value analysis, three alternative forms of the FLTA are envisaged; these are based on: peak values, short-term extremes and up-crossing rates. The FLTA is based on the total probability theorem and integrates the product of short-term probability distribution of the response parameter (peaks, extremes or up-crossing rate) and the probability distribution of the short-term environmental parameters to find the long-term probability distribution of the response. Thus, the full long-term analysis requires a significant amount of simulations for many environmental conditions. It also requires a sufficiently large sample to achieve good short-term statistics of the response. Hence, the FLTA is time consuming. Since extreme values mainly depend on the behaviour of the tail of its probability distribution, only a few environmental conditions actually contribute to the long-term result. For this reason, simplified methods have been proposed. These include the environmental contour method (ECM) discussed by Haver and Winterstein (2008) and simplified full long-term analysis (SLTA) (Videiro and Moan, 1999; Li *et al.*, 2016).

The ECM is based on determining the extreme short-term response for a set of environmental conditions on the contour line (for two parameters, such as H_s and T_p) or surface (for three parameters, such as H_s, T_p and U_w) of environmental conditions with a desired return period (50 years or 20 years etc.). The contour line or surface is determined by the inverse first order reliability method (IFORM). The actual long-term maximum is then obtained as the largest of the short term maxima. However, the ECM ignores the effect of the variability of the short-term response and compensates for this effect by using a higher fractile or the expected maxima multiplied by a factor larger than 1.0. Thus, the ECM requires that the true important environmental conditions be near the contour (Winterstein *et al.*, 1993; Muliawan *et al.*, 2013). To satisfy this requirement, however, it is found that the response should be a monotonic function of the environmental parameters. Thus, ECM does not perform well for wind turbines or other systems that have an on/off feature depending on the environment condition (Saranyasoontorn and Manuel, 2004; Agarwal and Manuel 2009; Li *et al.*, 2014). For bottom-fixed offshore wind turbines, a modification of the ECM is required by selecting an appropriate environmental contour with maximum wind speed within the operational range and using statistical extrapolation to find the long-term extreme of the desired return period.

SLTA is the same as FLTA except that it only includes the important environmental conditions and ignores those that do not contribute much to the long-term extremes. For a bottom-fixed wind turbine, it is found that less than 10 % of all the environmental

conditions are required to be simulated to achieve practically the same result as the FLTA (Li *et al.*, 2016).

4.7.3 Experimental Analysis of OWTs

In addition to numerical analysis, physical experimental methods can be used to gain further insight into the loads and responses of OWTs. Physical methods can include full-scale tests and measurements of components or systems, as well as small-scale experiments in controlled environments. Full-scale laboratory tests of components such as generators or blades are more commonly carried out than large scale support structure tests, although support structure data may be collected from demonstration projects at large scale in natural (uncontrolled) environments. This section focuses on small-scale tests, which include the support structure; as such, pure aerodynamic testing of the blades and rotor is not considered.

Small-scale tests for OWT support structures include tests that consider only hydrodynamic loading, as well as combined wind-wave (and wind-current) tests, which include the complete system. The design of such an experiment (or model test) depends on the objective of the test. Typical reasons for performing model tests include (Nielsen, 2012):

- confirming system behaviour;
- estimating extreme responses;
- evaluating nonlinear phenomena;
- performing a detailed load assessment;
- validating computer codes;
- convincing decision makers;
- understanding fluid flow phenomena.

For example, wave tank testing is an important tool for understanding nonlinear wave loading and wave-induced response of bottom-fixed wind turbines. The relevant wave conditions generally correspond to high wind speeds beyond cut-out, such that including the rotor is not considered to be of primary importance. Such a test resembles traditional offshore testing and Froude scaling is appropriate. For a geometrically scaled model, Froude scaling maintains the ratio between inertial and gravitational loads. The velocity (V), length (l) and acceleration due to gravity (g) define the scaling relationship between model (m) and prototype (p):

$$Fr = \frac{V_m}{\sqrt{g_m l_m}} = \frac{V_p}{\sqrt{g_p l_p}} \tag{4.13}$$

For a geometrically scaled model with $\lambda = l_m / l_p$, carried out in the same gravitational field, the velocity scale is thus $\lambda^{1/2}$, that is, velocities at model scale are reduced. Froude scaling is convenient for generating gravity waves (and practical due to the velocity reductions at model scale) but presents two important challenges with regards to model testing of OWTs: for flexible structures, elastic scaling is challenging, and Froude scaling implies a mismatch in Reynolds number.

Tests with flexible models are useful for understanding the responses of bottom-fixed wind turbines. In order to judge the importance of various wave conditions for the structure, it is useful to measure the response of a flexible model with the correct mode shapes and scaled natural period (de Ridder *et al*., 2011; Bredmose *et al*., 2013). For a flexible model, a softer material has to be used at model scale in order to match the mode shape and natural period. This can be observed by considering a cantilevered beam with Young's modulus E, constant cross-sectional area moment of inertia I, length L, and mass per length m. The deflection due to a point load (which is scaled with λ^3 following Froude scaling) should be scaled by λ, while the natural period should be scaled by $\sqrt{\lambda}$. Since geometrical scaling will give $m \propto \lambda^2$ and $I \propto \lambda^4$, it is trivial to show that $E_m = \lambda E_p$ is required. This is a challenge that can be addressed by changes in the geometry (such as the distribution of thickness) or by careful choice of material and mass distribution.

The second challenge – the mismatch in Reynolds number – is more difficult to address. The Reynolds number (Re) is the ratio between inertial and viscous forces:

$$Re = \frac{\rho V l}{\mu} \tag{4.14}$$

where ρ is the fluid's density and μ is the dynamic viscosity. Assuming that the same fluid is used at model and prototype scales, Re scales with $\lambda^{3/2}$: for a 1:50 scale model, the Reynolds number is too small by a factor of 353. The consequences of this difference are important to account for in both purely hydrodynamic tests and in combined wind-wave tests. In purely hydrodynamic tests, the differences in drag force due to a different Re regime can cause overestimation of damping or viscous excitation. For large volume structures and for structures with sharp corners – which trigger similar fluid behaviour at both scales – the impact may be small. For jacket structures or braces of semi-submersible structures, numerical validations should be carried out based on the model at small scale, while numerical analysis of the full-scale design should account for the full-scale drag coefficients.

In combined wind-wave tests, the aerodynamic performance of a wind turbine is severely affected by Re: aerofoil performance at different Re is not consistent. Carrying out a geometrically Froude-scaled test has been shown to give poor results: the thrust force is severely underpredicted, which makes results for the global performance of a FWT difficult to interpret (Robertson *et al*., 2013a). Alternative test methods include nongeometric scaling of the rotor and hybrid testing techniques.

Nongeometric rotor testing encompasses both drag-disk testing and performance-scaled rotors (Figure 4.15). For drag-disk testing, Froude-scaled wind (from fans) is applied to a large disk that is sized to give the correct mean Froude-scaled 'thrust' force. Some aerodynamic damping can be obtained, as well as gyroscopic forces if there is a spinning rotor (Roddier *et al*., 2010; Wan *et al*., 2015). Another alternative is to modify the wind turbine aerofoil shape and chord length in order improve performance at low Reynolds numbers. Improvements to the performance of a 1:50 scale 5-MW wind turbine in a wave basin have been documented but it remains challenging to simultaneously match the Froude-scale thrust, torque and slope of the thrust curve adequately with Froude-scaled wind (Fowler *et al*., 2013; Bottasso *et al*., 2014;

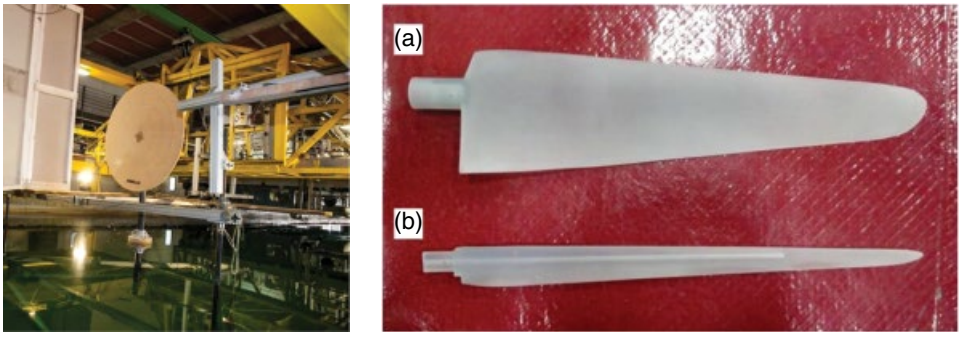

Figure 4.15 Nongeometric rotor scaling. Left: drag-disk tests of a combined wind and wave energy converter (Image from Ling Wan (Wan, 2014)). Right: (a) performance-scaled low Reynolds number blade; (b) corresponding geometrically scaled blade (*Source:* Kimball *et al*., 2014).

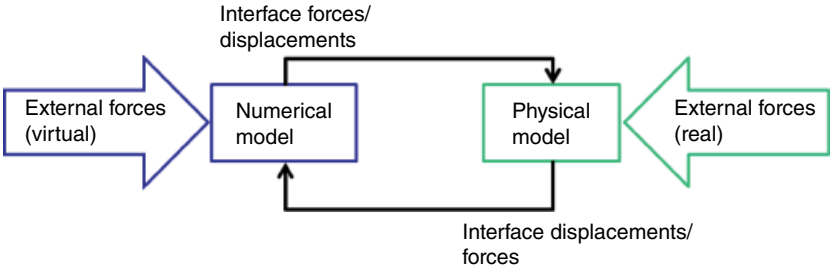

Figure 4.16 Hybrid testing (Chabaud *et al*., 2013; Hall *et al*., 2014; Bachynski *et al*., 2015, 2016; Sauder *et al*., 2016).

Kimball *et al*., 2014). Modelling the control system (such as active blade pitch) is challenging and it is not trivial to generate a high quality wind field in a wave basin. Numerical code validation using tests with non-geometrically-scaled rotors can also be difficult due to three-dimensional effects at low Reynolds numbers (Fernandes *et al*., 2014).

Recently, hybrid testing methods (Figure 4.16) have also gained traction as an alternative for wind-wave testing. In general, hybrid testing (also known as software-in-the-loop, hardware-in-the-loop or real-time hybrid model testing) consists of a combination of a physical model, which is subjected to physical loads, and a numerical model, which is run in real-time with feedback from measurements of the physical model and is used as the basis for actuating additional loads or motions. In the case of FWTs in the wave basin, the physical model may consist of the support structure and a mass model of the turbine, while the numerical model is used to calculate aerodynamic and generator loads.

The primary advantages of hybrid testing are that the scaling difficulties are avoided, the aerodynamic loads are known and the numerical model is flexible (i.e., it is possible to easily change from one turbine model to another, or incorporate changes in control). Of course, these tests are primarily applicable if the purpose of the model test is to confirm system behaviour, convince decision makers, or to study purely hydrodynamic

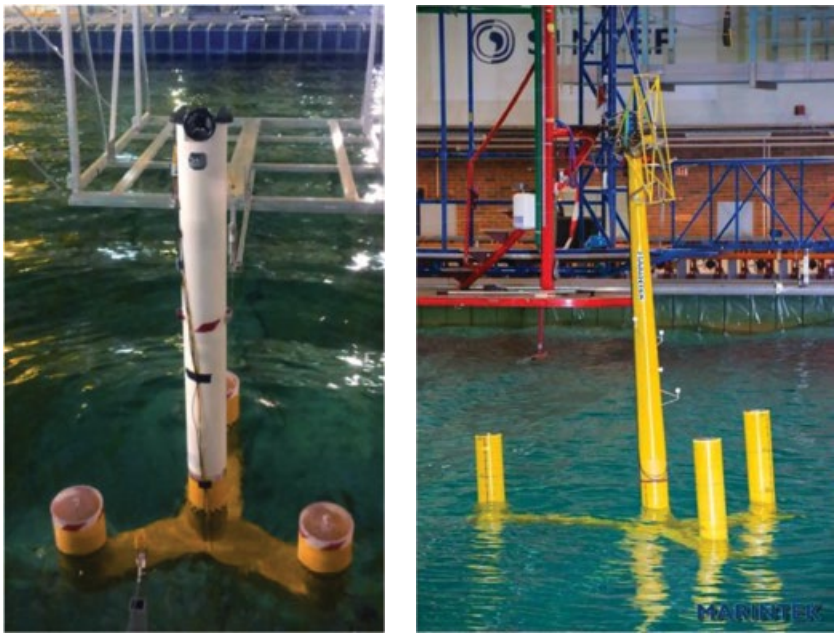

Figure 4.17 Real-time hybrid model tests of floating wind turbines. Left: ducted fan approach (*Source:* Azcona *et al*., 2014, http://iopscience.iop.org/article/10.1088/1742-6596/524/1/012089/meta. Used under CC BY licence (http://creativecommons.org/licenses/by/3.0/.); right: actuator approach (Bachynski *et al*., 2016).

phenomena. The first published hybrid wind-wave tests of a FWT focused primarily on the thrust force (Azcona *et al*., 2014) and applied forces on the model using a ducted fan. Later studies have also considered non-thrust loads and applied forces using alternative types of actuators (Bachynski *et al*., 2015, 2016; Sauder *et al*., 2016). Examples of such models are shown in Figure 4.17. Research challenges remain in the development of these test methods: further analysis of the frequency bandwidth, time delays in the system, actuator control and limitations on computational fidelity is needed. Parallel development of similar methods in wind tunnels is also underway (Bayati *et al*., 2013).

4.8 Conclusions

There is a significant variety and breadth in the design of support structures for OWTs: the best solution for a given site is highly dependent on the water depth, turbine size, geotechnical aspects and environmental conditions. Bottom-fixed structures, especially monopiles, dominate commercial projects at present, but significant research and development activities have been carried out on FWTs, which are expected to be economically viable in deeper water.

The support structure of an OWT is subjected to complex and coupled dynamic loads; aerodynamic and hydrodynamic effects have been briefly described. Design and

analysis methods for support structures therefore require consideration of the system as a whole. Numerical aero-hydro-servo-geo-elastic analysis tools as well as experimental methods have been developed to better understand the behaviour of OWTs in general, and support structures in particular.

4.9 References

ABS (American Bureau of Shipping) (2013) *Guide for building and classing floating offshore wind turbine installations*. ABS, Houston, TX.

Agarwal, P. and Manuel, L. (2009) Simulation of offshore wind turbine response for long-term extreme load prediction. *Engineering Structures*, **31** (10), 2236–2246.

Azcona, J., Bouchotrouch, F., González, M. *et al*. (2014) Aerodynamic Thrust Modelling in Wave Tank Tests of Offshore Floating Wind Turbines using a Ducted Fan. *Journal of Physics: Conference Series, The Science of Making Torque from Wind 2014*, **524**, 012089.

Bachynski, E.E. (2014) Design and dynamic analysis of tension-leg platform wind turbines. PhD thesis, Norwegian University of Science and Technology.

Bachynski, E.E. and Moan, T. (2012) Design considerations for tension-leg platform wind turbines. *Marine Structures*, **29**, 89–114.

Bachynski, E.E. and Moan, T. (2014a) Ringing loads on tension-leg platform wind turbines. *Ocean Engineering*, **84**, 237–248.

Bachynski, E.E. and Moan, T. (2014b) Second order wave force effects on tension-leg platform wind turbines in misaligned wind and waves. *33rd International Conference on Ocean, Offshore and Arctic Engineering Volume 9A: Ocean Renewable Energy*, San Francisco, CA.

Bachynski, E.E., Etemaddar, M., Kvittem, M.I. *et al*. (2013) Dynamic analysis of floating wind turbines during pitch actuator fault, grid loss, and shutdown. *Energy Procedia*, **35**, 210–222.

Bachynski, E.E., Kvittem, M.I., Luan, C. and Moan, T. (2014) Wind-wave misalignment effects on floating wind turbines: motions and tower load effects. *Journal of Offshore Mechanics and Arctic Engineering*, **136** (4), 041902.

Bachynski, E.E., Chabaud, V. and Sauder, T. (2015) Real-time hybrid model testing of floating wind turbines: sensitivity to limited actuation. *Energy Procedia*, **80**, 2–12.

Bachynski, E.E., Thys, M., Sauder, T. *et al*. (2016) Real-time hybrid model testing of a braceless semi-submersible wind turbine: Part II: Experimental Results, in *Proceedings of the ASME 2016 35th International Conference on Ocean, Offshore and Arctic Engineering*, Busan, South Korea.

Bae, Y.H., Kim, M.H., Im, S.W. and Chang, I.H. (2011) Aero-elastic-control-floater-mooring coupled dynamic analysis of floating offshore wind turbines, in *Proceedings of the Twenty-first (2011) International Offshore and Polar Engineering Conference*, Maui, HI, 19–24 June, pp. 429–435.

Bayati, I., Belloli, M., Facchinetti, A. and Giappino, S. (2013) Wind tunnel tests on floating offshore wind turbines: a proposal for hardware-in-the-loop approach to validate numerical codes. *Wind Engineering*, **37** (6), 557–568.

Bjørgum, A. (2015) Life cycle cost analysis for corrsion protective coatings -offshore wind turbines, in *Life Cycle Costing. For the Analysis, Management and Maintenance of Civil Engineering Infrastructure* (ed J.W. Bull), Whittles Publishing, Dunbeath, UK., 210–230.

Borg, M., Hansen, A.M. and Bredmose, H. (2016) Floating substructure flexibility of large-volume 10 MW offshore wind turbine platforms in dynamic calculations. *Journal of Physics: Conference Series*, **753** (8), 082024.

Botta, G., Casale, C., Lembo, E. *et al.* (2009) Resource and technology assessment for evaluating Italy's offshore wind energy potential, in *International Conference on Clean Electrical Power*, June, pp. 507–513.

Bottasso, C.L., Campagnolo, F. and Pectrović, V. (2014) Wind tunnel testing of scaled wind turbine models: Beyond aerodynamics. *Journal of Wind Engineering and Industrial Aerodynamics*, **127**, 11–28.

Bredmose, H., Sahlberg-Nielsen, L., Slabiak, P. and Schütter, F. (2013) Dynamic excitation of monopiles by steep and breaking waves. Experimental and numerical study, in *ASME 2013 32nd International Conference on Ocean, Offshore and Arctic Engineering*, Nantes, France, 9–14 June.

Burton, T., Jenkins, N., Sharpe, D. and Bossanyi, E. (2011) *Wind Energy Handbook*, John Wiley & Sons Ltd, Chichester.

Chabaud, V., Steen, S. and Skjetne, R. (2013) Real-time hybrid testing for marine structures: challenges and strategies, in *ASME 2013 32nd International Conference on Ocean, Offshore and Arctic Engineering*, Nantes, France, 9–14 June.

Chakrabarti, S.K. (ed) (2005) *Handbook of Offshore Engineering*, Elsevier Science.

Chakrabarti, S.K. and Hanna, S.Y. (1990) Added mass and damping of a TLP column model, in *22nd Annual Offshore Technology Conference*, Houston, TX, pp. 559–571.

Chen, X. and Yu, Q. (2013) *Design guideline for stationkeeping systems of FOWT*. American Bureau of Shipping, Houston, TX.

Chen, I.-W., Wong, B.-L., Lin, Y.-H. *et al.* (2016) Design and analysis of jacket substructures for offshore wind turbines. *Energies*, **9** (4), 264.

Clauss, G., Lehmann, E., Ostergaard, C. and Shields, M.J. (1982) *Offshore Structures: Conceptual Design and Hydromechanics*, Springer-Verlag.

Cook, R.D., Malkus, D.S., Plesha, M.E. and Witt, R.J. (2002) *Concepts and Applications of Finite Element Analysis*, 4th edn, John Wiley & Sons Ltd, Chichester.

Coulling, A.J., Goupee, A.J., Robertson, A.N. and Jonkman, J. (2013) Importance of second-order difference-frequency wave diffraction forces in the validation of a FAST semi-submersible floating wind turbine model, in *ASME 2013 32nd International Conference on Ocean, Offshore and Arctic Engineering*, Nantes, France, 9–14 June.

Crozier, A. (2011) *Design and dynamic modeling of the support structure for a 10 MW offshore wind turbine*. Masters thesis, NTNU (Norwegian University of Science and Technology).

de Ridder, E.-J., Aalberts, P., van den Berg, J. *et al.* (2011) The dynamic response of an offshore wind turbine with realistic flexibility to breaking wave impact, in *ASME 2011 30th International Conference on Ocean, Offshore and Arctic Engineering*, Rotterdam, the Netherlands.

DNV (Det Norske Veritas) (2007) Design of Offshore Wind Turbine Structures.

DNV (Det Norske Veritas) (2010a) Environmental Conditions and Environmental Loads.

DNV (Det Norske Veritas) (2010b) Fatigue Design of Offshore Steel Structures.

DNV (Det Norske Veritas) (2013) Design of Floating Wind Turbine Structures.

Doherty, P., Gavin, K. and Casey, B. (2011) The Geotechnical Challenges Facing the Offshore Wind Sector, in *Geo-Frontiers 2011*, American Society of Civil Engineers, 162–171.

Dudgeon Offshore Wind Farm (2014) Dudgeon offshore wind farm awards monopile foundations fabrication contract, http://dudgeonoffshorewind.co.uk/news/news-04-07-14-2 (last accessed 5 July 2017).

Etemaddar, M., Hansen, M.O.L. and Moan, T. (2014) Wind turbine aerodynamic response under atmospheric icing conditions. *Wind Energy*, **17** (2), 14.

EWEA (European Wind Energy Association) (2016) The European offshore wind industry key trends and statistics 2015, http://www.ewea.org/fileadmin/files/library/publications/statistics/EWEA-European-Offshore-Statistics-2015.pdf (last accessed 5 July 2017).

Faltinsen, O.M. (1990) *Sea Loads on Ships and Offshore Structures*, Cambridge University Press.

Fernandes, G., Make, M., Gueydon, S. and Vaz, G. (2014) Sensitivity to aerodynamic forces for the accurate modelling of floating offshore wind turbines, in *RENEW2014* (ed G. Soares). doi: 10.13140/2.1.3656.1600.

Fowler, M.J., Kimball, R.W., Thomas, D.A. and Goupee, A.J. (2013) Design and testing of scale model wind turbines for use in wind/wave basin model tests of floating offshore wind turbines, in *ASME 2013 32nd International Conference on Ocean, Offshore and Arctic Engineering*, Nantes, France, 9–14 June.

Fylling, I. and Berthelsen, P.A. (2011) WINDOPT – an optimization tool for floating support structures for deep water wind turbines, in *30th International Conference on Ocean, Offshore and Arctic Engineering*, Rotterdam, the Netherlands.

Goupee, A.J., Fowler, M.J., Kimball, R.W. *et al*. (2014) Additional wind/wave basin testing of the DeepCwind semisubmersible with a performance-matched wind turbine, in *Proceedings of the ASME 2014 33rd International Conference on Ocean, Offshore and Arctic Engineering OMAE2014*, San Francisco, CA.

Gravesen, H., Sørensen, S.L., Vølund, P. *et al*. (2005) Ice loading on Danish wind turbines: Part 2. Analyses of dynamic model test results. *Cold Regions Science and Technology*, **41**, 25–47.

Hall, M., Moreno, J. and Thiagarajan, K. (2014) Performance specifications for real-time hybrid testing of 1:50-scale floating wind turbine models, in *Proceedings of the ASME 2014 33rd International Conference on Ocean, Offshore and Arctic Engineering OMAE2014*, San Francisco, CA.

Hansen, M.O.L., Sørensen, J.N., Voutsinas, S. *et al*. (2006) State of the art in wind turbine aerodynamics and aeroelasticity. *Progress in Aerospace Sciences*, **42** (4), 285–330.

Haver, S. and Winterstein, S.R. (2008) Environmental contour lines: a method for estimating long term extremes by a short term analysis. *Transactions of the Society of Naval Architects and Marine Engineers*, **116**, 12.

Henderson, A.R., Argyriadis, K., Nichos, J. and Langston, D. (2010) Offshore wind turbines on TLPs – Assessment of floating support structures for offshore wind farms in German waters, in *10th German Wind Energy Conference*, Bremen, Germany.

Hibbeler, R.C. (2005) *Mechanics of Materials*, Prentice Hall.

IDEOL (2016) *IDEOL winning solutions for offshore wind* [online]. https://ideol-offshore.com/sites/default/files/pdf/ideol_-_press_kit.pdf; last accessed 28 July 2017).

IEC (International Electrotechnical Commission) (2005) *Wind turbines: Part 1: Design Requirements*. IEC, Geneva.

IEC (International Electrotechnical Commission) (2009) *Wind turbines: Part 3: Design requirements for offshore wind turbines*. IEC, Geneva.

Jain, R.K. (1980) A simple method of calculating the equivalent stiffnesses in mooring cables. *Applied Ocean Research*, **2** (3), 139–142.

Jiang, Z., Karimirad, M. and Moan, T. (2013) Dynamic response analysis of wind turbines under blade pitch system fault, grid loss and shut down events. *Wind Energy*, **17** (9), 1385–1409.

Jonkman, B.J. (2009) *TurbSim User's Guide: Version 1.50*. National Renewable Energy Laboratory, Golden, CO.

Jonkman, J., Butterfield, S., Musial, W. and Scott, G. (2009) *Definition of a 5-MW reference wind turbine for offshore system development*. National Renewable Energy Laboratory, Golden, CO.

Karimirad, M. (2011) Stochastic dynamic response analysis of spar-type wind turbines with catenary or taut mooring systems. PhD thesis, Norwegian University of Science and Technology.

Karimirad, M. and Michailides, C. (2015) V-shaped semisubmersible offshore wind turbine: An alternative concept for offshore wind technology. *Renewable Energy*, **83**, 126–143.

Karimirad, M. and Moan, T. (2011) Wave- and wind-induced dynamic response of a spar-type offshore wind turbine. *Journal of Waterway, Port, Coastal, and Ocean Engineering*, **138** (1), 9–20.

Kimball, R., Goupee, A.J., Fowler, M.J. *et al.* (2014) Wind/wave basin verification of a performance-matched scale-model wind turbine on a floating offshore wind turbine platform, in *Proceedings of the ASME 2014 33rd International Conference on Ocean, Offshore and Arctic Engineering OMAE2014*, San Francisco, CA.

Koo, B., Goupee, A.J., Lambrakos, K. and Lim, H.-J. (2014) Model test data correlations with fully coupled hull/mooring analysis for a floating wind turbine on a semi-submersible platform, in *Proceedings of the ASME 2014 33rd International Conference on Ocean, Offshore and Arctic Engineering OMAE2014*, San Francisco, CA.

Krolis, V.D., van der Zwaag, G.L. and de Vries, W. (2010) Determining the embedded pile length for large-diameter monopiles. *Marine Technology Society Journal*, **44** (1), 24–31.

Kvittem, M.I. and Moan, T. (2015) Frequency versus time domain fatigue analysis of a semisubmersible wind turbine tower. *Journal of Offshore Mechanics and Arctic Engineering*, **137**, 11.

Kvittem, M.I., Moan, T., Gao, Z. and Luan, C. (2011) Short-term fatigue analysis of semi-submersible wind turbine tower, in *30th International Conference on Ocean, Offshore, and Arctic Engineering*, Rotterdam, the Netherlands.

Larsen, T.J. and Hanson, T.D. (2007) A method to avoid negative damped low frequent tower vibrations for a floating, pitch controlled wind turbine. *Journal of Physics: Conference Series, The Second Conference on The Science of Making Torque from Wind*, Vol. **75**.

Li, Q., Gao, Z. and Moan, T. (2014) Extreme response analysis for a jacket-type offshore wind turbine using environmental contour method, in *Safety, Reliability, Risk and Life-Cycle Performance of Structures and Infrastructures* (eds G. Deodatis, B.R. Ellingwood and D.M. Frangopol), CRC Press, pp. 5597–5604.

Li, Q., Gao, Z. and Moan, T. (2016) Modified environmental contour method for predicting long-term extreme responses of bottom-fixed offshore wind turbines. *Marine Structures*, **48**, 15–32.

Lotsberg, I. (2013) Structural mechanics for design of grouted connections in monopile wind turbine structures. *Marine Structures*, **32**, 113–135.

Luan, C., Gao, Z. and Moan, T. (2016) Design and analysis of a braceless steel 5-MW semi-submersible wind turbine, in *Proceedings of the ASME 2016 35th International Conference on Ocean, Offshore and Arctic Engineering*, Busan, South Korea.

Mann, J. (1998), Wind field simulation. *Probabilistic Engineering Mechanics*, **13** (4), 269–282.

Manwell, J.F., McGowan, J.G. and Rogers, A.L. (2009) *Wind Energy Explained*, John Wiley & Sons Ltd, Chichester.

Masciola, M., Chen, X. and Yu, Q. (2015) Evaluation of the dynamic-response-based intact stability criterion for floating wind turbines, in *34th International Conference on Ocean, Offshore and Arctic Engineering*, St John's, NF, Canada.

Matha, D. (2009) *Model development and loads analysis of an offshore wind turbine on a tension-leg platform, with a comparison to other floating turbine concepts*. University of Colorado-Boulder.

Moné, C., Smith, A., Maples, B. and Hand, M. (2015a) *2013 Cost of Wind Energy Review*. National Renewable Energy Laboratory, Golden, CO.

Moné, C., Stehly, T., Maples, B. and Settel, M. (2015b) *2014 Cost of Wind Energy Review*. National Renewable Energy Laboratory, Golden, CO.

Moon III, W.L. and Nordstrom, C.J. (2010) Tension-leg platform turbine: a unique integration of mature technologies, in *Proceedings of the 16th Offshore Symposium, Texas Section of the Society of Naval Architects and Marine Engineers*, pp. A25–A34.

Muliawan, M.J., Gao, Z. and Moan, T. (2013) Application of the contour line method for estimating extreme responses in the mooring lines of a two-body floating wave energy converter. *Journal of Offshore Mechanics and Arctic Engineering*, **135** (3), 031301.

Myhr, A., Maus, K.J. and Nygaard, T.A. (2011) Experimental and computational comparisons of the OC3-HYWIND and tension-leg-buoy (TLB) floating wind turbine conceptual designs, in *Proceedings of the Twenty-first (2011) International Offshore and Polar Engineering Conference*, Maui, HI, 19–24 June, pp. 353–360.

Naess, A. and Moan, T. (2013) *Stochastic Dynamics of Marine Structures*, Cambridge University Press.

Neumann, G. and Pierson, W.J., Jr (1966) *Principles of Physical Oceanography*, Prentice-Hall Inc, Eaglewood Cliffs, NJ.

Newman, J.N. (1977) *Marine Hydrodynamics*, The MIT Press, Cambridge, MA.

Nielsen, F.G. (2012) *Experts' Meeting on Computer Code Validation for Offshore Wind System Modeling. EA Wind Task 30*, Boulder, CO.

NORSOK (2007) Action and action effects. NORSOK Standard N-003, Standards Norway, Lysaker, Norway.

NORSOK (2012) *Surface preparation and protective coating. NORSOK Standard M-501*, Norwegian Technology Standards Institution, Oslo.

Nygaard, T.A. and Myhr, A. (2014) Tension-leg-buoy (TLB) platforms for offshore wind turbines, in *EERA DeepWind'2014 Deep Sea Offshore Wind R&D Conference*, Trondheim, Norway, 22–24 January, European Energy Research Alliance (EERA).

Ormberg, H. and Bachynski, E.E. (2015) Sensitivity of estimated tower fatigue to wind modeling for a spar floating wind turbine, in *The Twenty-fifth (2015) International Offshore and Polar Engineering Conference*, Kona, Big Island, HI.

Principle Power (2011) *WindFloat*. Principle Power Inc, http://www.principlepowerinc.com/en/windfloat (last accessed 5 July 2017).

Prowell, I. and Veers, P. (2009) *Assessment of wind turbine seismic risk: existing literature and simple study of tower moment demand*. Sandia National Laboratories, Albuquerque, NM / Livermore, CA.

Roald, L., Jonkman, J., Robertson, A. and Chokani, N. (2013) Effect of second-order hydrodynamics on floating offshore wind turbines. *Energy Procedia*, **35**, 253–264.

Robertson, A., Jonkman, J., Goupee, A.J. *et al*. (2013a) Summary of conclusions and recommendations drawn from the DeepCwind scaled floating offshore wind system test

campaign, in *Proceedings of the ASME 2013 32nd International Conference on Ocean, Offshore and Arctic Engineering*, Nantes, France, 9–14 June.

Robertson, A., Jonkman, J., Masciola, M. *et al.* (2012) *Definition of the semisubmersible floating system for Phase II of OC4*. National Renewable Energy Laboratory (NREL), Golden, CO.

Robertson, A., Jonkman, J., Musial, W. *et al.* (2013b) Offshore code comparison collaboration, continuation: Phase II results of a floating semisubmersible wind system, in *EWEA Offshore 2013*, Frankfurt, Germany, 19–21 November.

Roddier, D., Cermelli, C., Aubault, A. and Weinstein, A. (2010) WindFloat: A floating foundation for offshore wind turbines. *Journal of Renewable and Sustainable Energy*, **2** (3), 033104.

Roddier, D., Peiffer, A., Aubault, A. and Weinstein, J. (2011) A generic 5 MW windfloat for numerical tool validation & comparison against a generic spar, in *ASME 2011 30th International Conference on Ocean, Offshore and Arctic Engineering*, Rotterdam, the Netherlands.

Saranyasoontorn, K. and Manuel, L. (2004) On assessing the accuracy of offshore wind turbine reliability-based design loads from the environmental contour method, in *Fourteenth International Offshore and Polar Engineering Conference*, Toulon, France, pp. 128–135.

Sauder, T., Chabaud, V., Thys, M. *et al.* (2016) Real-time hybrid model testing of a braceless semi-submersible wind turbine: Part I: the hybrid approach, in *Proceedings of the ASME 2016 35th International Conference on Ocean, Offshore and Arctic Engineering*, Busan, South Korea.

Sherringham Shoal Offshore Wind Farm (2012) Green out of the blue. http://scira.co.uk/newsdownloads/Downloads/SSWOF%20Green%20out%20of%20blue%20AW%20web%209.12.pdf; last accessed 28 July 2017.

Shi, W., Tan, X., Gao, Z. and Moan, T. (2016) Numerical study of ice-induced loads and responses of a monopile-type offshore wind turbine in parked and operating conditions. *Cold Regions Science and Technology*, **123**, 121–139.

Statoil (2011) Hywind – the leading solution for floating offshore wind power. https://www.statoil.com/content/statoil/en/what-we-do/hywind-where-the-wind-takes-us.html; last accessed 28 July 2017.

Stokey, W.F. (1961) Vibration of systems having distributed mass and elasticity, in *Harris' Shock and Vibration Handbook* (eds C.M. Harris and A.G. Piersol), McGraw-Hill, New York.

Suzuki, K., Yamaguchi, H., Akase, M. *et al.* (2010) Initial design of TLP for offshore wind farm, in *Renewable Energy Conference 2010*, Yokohama, Japan.

SWAY (2012) *Changing the future of wind power*. SWAY AS, Bergen, Norway; http://www.sway.no/ (last accessed 5 July 2017).

The Engineer (2012) Wind energy gets serial. https://www.theengineer.co.uk/issues/30-april-2012/wind-energy-gets-serial/ (last accessed 5 July 2017).

Twidell, J. and Gaudiosi, G.(eds) (2009) *Offshore Wind Power*, Multi-Science Publishing Co, Brentwood, UK.

Utsunomiya, T., Matsukuma, H., Minoura, S. *et al.* (2010) On sea experiment of a hybrid spar for floating offshore wind turbine using 1/10 scale model, in ASME 2010 29th International Conference on Ocean, Offshore and Arctic Engineering, Shanghai, China, 6–11 June.

van der Tempel, J. (2006) *Design of support structures for offshore wind turbines*, Delft University of Technology.

Videiro, P. and Moan, T. (1999) Efficient evaluation of long-term distributions, in *18th International Conference on Offshore Mechanics and Arctic Engineering*, St John's, NF

Viselli, A.M., Goupee, A.J. and Dagher, H.J. (2014) Model test of a 1:8 scale floating wind turbine offshore in the Gulf of Maine, in *Proceedings of the ASME 2014 33rd International Conference on Ocean, Offshore and Arctic Engineering OMAE2014*, San Francisco, CA.

Wan, L., Gao, Z. and Moan, T. (2015) Experimental and numerical study of hydrodynamic responses of a combined wind and wave energy converter concept in survival modes. *Coastal Engineering*, **104**, 151–169.

Wienke, J. and Oumeraci, H. (2005) Breaking wave impact force on a vertical and inclined slender pile – theoretical and large-scale model investigations. *Coastal Engineering*, **52**, 435–462.

Winterstein, S.R., Ude, T.C., Cornell, C.A. *et al*. (1993) Environmental parameters for extreme response: Inverse FORM with omission factors, in *6th International Conference on Structural Safety and Reliability*, Innsbruck, Austria.

Zang, J., Taylor, P.H., Morgan, G. *et al*. (2010) Steep wave and breaking wave impact on offshore wind turbine foundations – ringing re-visited, in *International Workshop on Water Waves and Floating Bodies (IWWWFB25)*, Harbin, China, 9–12 May, pp. 193–196.

Zhao, Y., Yang, J. and He, Y. (2012) Preliminary Design of a multi-column TLP foundation for a 5-MW offshore wind turbine. *Energies*, **5**, 3874–3891.